ELSEVIER

Sedimentary Geology 145 (2001) 189–213

Sedimentary Geology

www.elsevier.com/locate/sedgeo

Genesis and geometry of the Meiklejohn Peak lime mud-mound, Bare Mountain Quadrangle, Nevada, USA: Ordovician limestone with submarine frost heave structures—a possible response to gas clathrate hydrate evolution

Federico F. Krause*

University of Calgary, Department of Geology and Geophysics, 2500 University Drive N.W., Calgary, Alberta, Canada T2N 1N4

Received 3 August 2000; accepted 15 May 2001

Abstract

During the Early Middle Ordovician (Early Whiterockian) the Meiklejohn Peak lime mud-mound, a large whaleback or dolphin back dome, grew on a carbonate ramp tens to hundreds of kilometres offshore. This ramp extended from the northwest margin of Laurentia into the open waters of the ancestral Pacific Ocean to the north. The mound developed in an outer ramp environment, in relatively deep and cold water. A steep northern margin with a slope that exceeds 55° characterizes the mound. This margin is split by a 14-m long vertical fracture that separates a zone of slumped, drag-folded and brecciated rocks from the main mass of the mound. Failure along this fracture occurred subcutaneously, as highlighted by covering beds that are folded next to the mound. Brecciated blocks and clasts contain zebra and stromatactis structures indicating that these rocks and structures were lithified early in the history of the mound. The southern end of the mound is less steep and is characterized by large, echinodermal grainstone cross-beds. These deposits are part of a large, subaqueous dune that grew northwards and preceded the main development of the mound. Southward dipping and downlapping layers of mud-mound mudstone and wackestone overlie the dune. These muddy limestone layers are cut in several places by injection dykes and are pierced, near the contact with the underlying dune, by a 25-m long pipe filled with rotated nodular and brecciated mud-mound clasts. This long pipe extends to the edge of the mound and appears to have been a conduit where fluidized materials that came from the mound's interior were vented.

The interior of the mound is typified by light grey limestone with zebra bands and stromatactis structures. Both structures represent former cavity systems that are filled with fibrous and bladed calcite and pelleted and laminated geopetal mudstone. Spar bands of zebra limestone often extend for several metres and appear to have been unsupported over these distances. Zebra banded rocks are also accompanied by snout and socket structures and, in some instances, are folded and sheared by curving kink bands. Zebra and stromatactis limestone structures found throughout the mud-mound resemble frost heave and cryoturbation structures identified in both Holocene and Pleistocene cryosols, and in laboratory experiments with advancing freezing fronts in clay-size sediment. Significantly, modern occurrences of methane clathrate hydrate (methane-charged ice) display parallel and digitate layering similar in depositional appearance to that of zebra and stromatactis limestone from Meiklejohn Peak. Early carbonate cements are also commonly associated with these modern clathrate hydrate deposits. Consequently, gas clathrate hydrates may have been the propping agent for zebra and stromatactis structures observed in the

* Fax: +1-403-284-0074.
E-mail address: krause@geo.ucalgary.ca (F.F. Krause).

PII: S0037-0738(01)00148-8

mud-mound. In this scenario, carbonate cements would have precipitated and stabilized these structures, both with the consolidation and dissociation of gas clathrate hydrates, and with the oxidation and reduction of associated gases. Stable $\delta^{13}C$ and $\delta^{18}O$ isotope ratios collected from mudstone and spar of zebra and stromatactis structures indicate that they were lithified in equilibrium with Ordovician seawater. The $\delta^{13}C$ isotope ratios recorded at Meiklejohn Peak are similar to $\delta^{13}C$ isotopic ratios obtained from $\sum CO_2$ evolving from modern seafloor. These isotopic ratios may indicate that frost heave structures in the Meiklejohn Peak mud-mound are the result of consolidation and dissociation of carbon dioxide clathrate hydrates. Even though the bulk of gas clathrate hydrates identified to date in modern ocean floors are composed of methane, carbon dioxide clathrate hydrates are known from the modern seafloor of the Okinawa Trough. They may also be common in areas of abundant carbonate sediment accumulation, as suggested by recent observations from the Great Australian Bight.

Keywords: Mud-mound; Meiklejohn Peak; Stromatactis and zebra structures; Frost heave; Gas clathrate hydrates; Carbon and oxygen isotopes

1. Introduction

The Meiklejohn Peak carbonate mud-mound is a conspicuous dome located on the western slopes of Bare Mountain, Nevada (Figs. 1 and 2) (Cornwall and Kleinhampl, 1961; Krause, 1974; Krause and Rowell, 1975; Ross et al., 1975, 1989; James, 1983). Easily seen from Secret Pass, it is located approximately 11 km to the east of the town of Beatty. The Meiklejohn Peak mound is one of three mud-mounds that have been reported in Ordovician strata in Nevada (Fig. 3) (Ross and Cornwall, 1961; Cornwall and Kleinhampl, 1961). The other two occur to the east of Meiklejohn Peak: one, southwest of Aysees Peak in the Frenchman Lake Quadrangle, and the other, west of Oak Spring in the northern part of the Tippipah Spring Quadrangle (Fig. 1) (Ross and Cornwall, 1961). Only the mound at Meiklejohn Peak is readily accessible as good desert roads lead to within a few hundred metres of its base (Fig. 2). The other two mounds are in restricted access areas, one being a bombing range, the other the Nevada Test Site (Fig. 1). The Meiklejohn Peak carbonate mud-mound is contained in the lower Antelope Valley Limestone and situated biostratigraphically within brachiopod Zone L (*Orthidiella* Zone), near the base of the North American, Whiterock Series of the Ordovician System (Ross et al., 1975; Ross and Ethington, 1991).

Major features of the structural history of the Bare Mountain Quadrangle have been summarized by Cornwall and Kleinhampl (1961). In the vicinity of Meiklejohn Peak, Bare Mountain is characterized by a series of imbricated thrust plates. Formations and groups ranging in age from Cambrian through Mississippian are cut by these thrusts, and are juxtaposed in variable stratigraphic order as a result of this deformation. The Ordovician Pogonip Group, in which the carbonate mud-mound is located, and the Eureka Quartzite and Ely Springs Dolostone are thrust over the Devonian Flourspar Canyon Formation which, in turn, is thrust over the Mississippian Meiklejohn and Cambrian Carrara Formations. In the immediate vicinity of the mound, beds above and below dip steeply to the east, dip 50–52°, dip direction 42–47°; Cornwall and Kleinhampl (1961) report a slightly lower dip 45°, but a similar dip direction. Exposed on the western flanks of Meiklejohn Peak are Ordovician rocks that comprise the Pogonip Group, which in stratigraphic younging order includes the Goodwin Limestone, Nine Mile and Antelope Valley Limestone Formations (Fig. 4). Overlying this group are the Eureka Quartzite and Ely Springs Dolostone (Fig. 4). These rocks encompass all the Ordovician Series, but include several unconformities with time spans of variable duration; the widest and most extensive spans occur well above the mud-mound at the top of the Antelope Valley Limestone and Eureka Quartzite formations, respectively (Ross et al., 1989).

Following the initial mapping reports by Cornwall and Kleinhampl (1961) and Ross and Cornwall (1961), the Meiklejohn Peak mud-mound has attracted a variety of geological studies (Ross, 1972; Krause, 1974, 1999, 2000; Krause and Rowell, 1975; Krause and Sayegh, 2000; Ross et al., 1975; Bathurst, 1977; James, 1983; Pratt, 1995; Tobin and Walker, 1995). The mud-mound and less commonly strati-

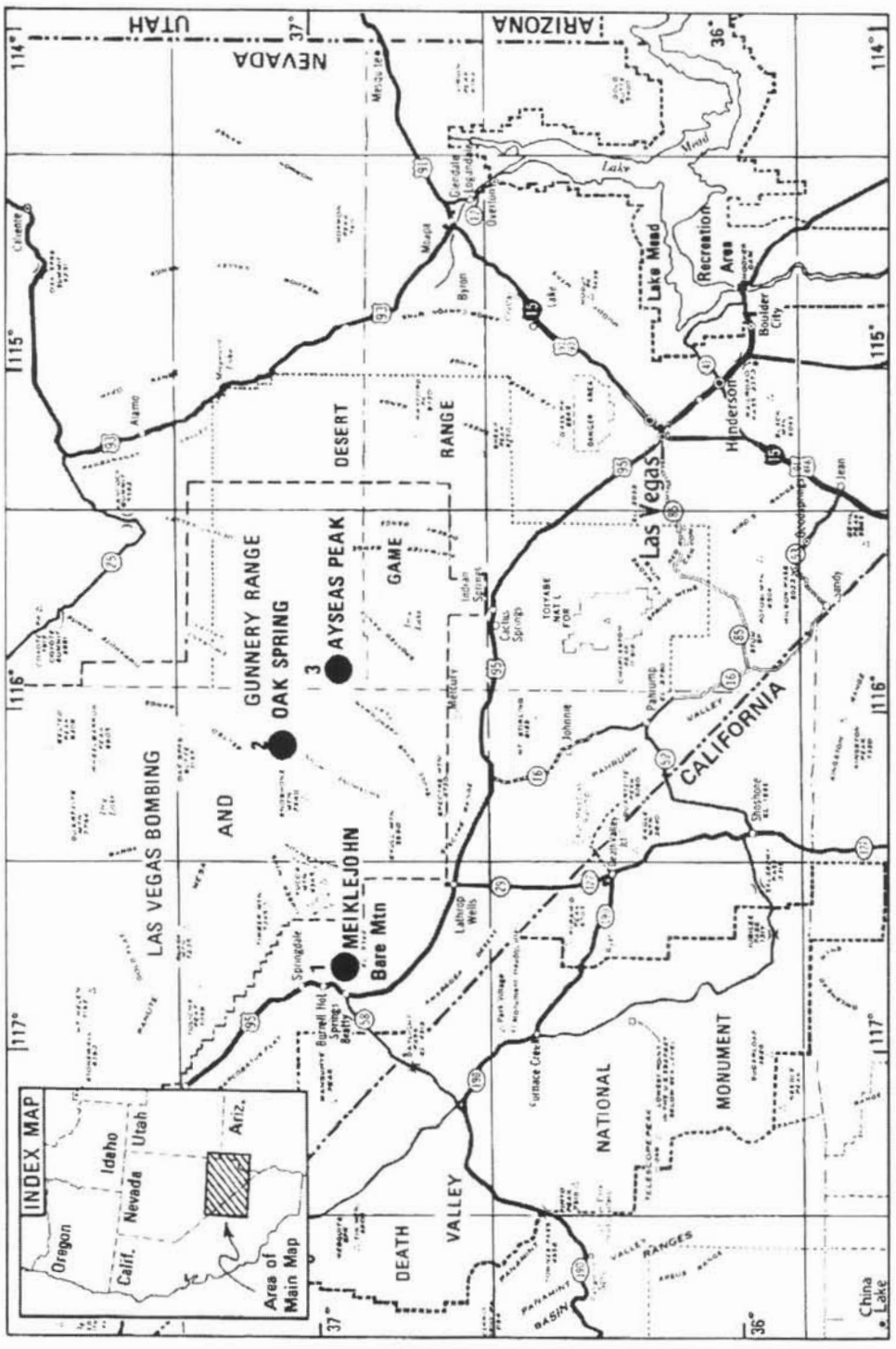

Fig. 1. Regional index and location maps highlighting sites of Ordovician mud-mounds identified in southern Nevada (Cornwall and Kleinhampl, 1961; Ross and Cornwall, 1961). Bare Mountain is the location for the Meiklejohn Peak carbonate mud-mound. Meiklejohn Peak is due east from the town of Beatty and approximately 10 km away.

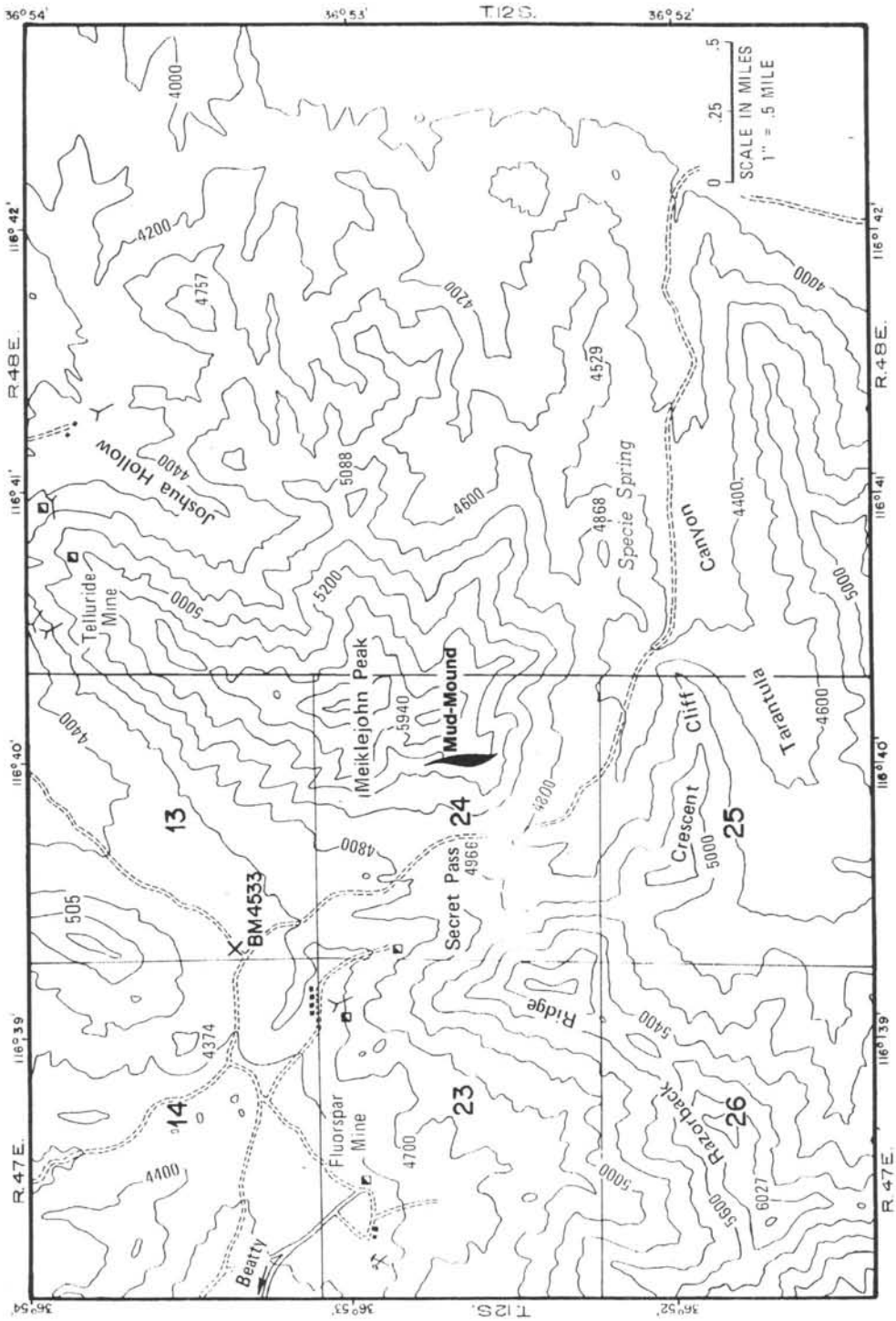

Fig. 2. Topographic map of the Meiklejohn Peak area illustrating the location of the mud-mound and road access to Secret Pass (based on the map of Cornwall and Kleinhampl, 1961).

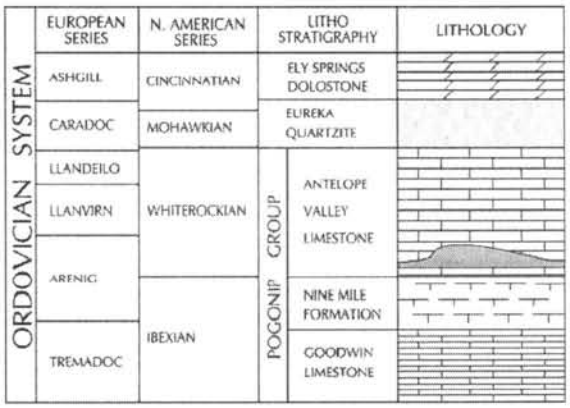

Fig. 3. Lithostratigraphic, chronostratigraphic and lithologic chart of Ordovician System rocks in the Meiklejohn Peak area (after Cornwall and Kleinhampl, 1961; Ross 1964, 1972; Ross and Ethington, 1991; Sprinkle and Guensburg, 1995).

graphically adjacent rocks contain remarkable deposits of zebra and stromatactis limestone, which were the focus of the study by Ross et al. (1975). The two principal aims of this report are to highlight characteristics of the depositional geometry of the mound that have not been noted in previous studies, and to establish the genesis of the mound from the zebra and stromatactis limestone that dominate its bulk.

2. The Meiklejohn Peak carbonate mud-mound

2.1. Regional stratigraphy and depositional setting

The Meiklejohn Peak mud-mound is a minuscule dot relative to the vast carbonate platform on which it once existed. This platform, at least 450 km wide and 1100 km in length, covered the same area presently occupied by Utah, Nevada and south eastern California and lasted approximately 12 Ma during the Middle Ordovician (Late Arenigian through Llanvirn and Llandeilo time) (Ross et al., 1989). In the global paleogeographic reconstruction of the Middle Ordovician by Dalziel (1997), the carbonate platform would have projected into the ancestral Pacific Ocean at approximately 30°N latitude, on the north margin of the Laurentia Continent. This continental margin conformed coarsely to the outline of the present western margin of North America, but was oriented east to west and situated hundreds of kilometres inboard of the present margin. Thus, on this platform, the Meiklejohn Peak mud-mound would have faced the open waters of an ancestral Pacific Ocean to the north.

During the 12 Ma of its existence, the platform on which the Meiklejohn Peak mud-mound was situated

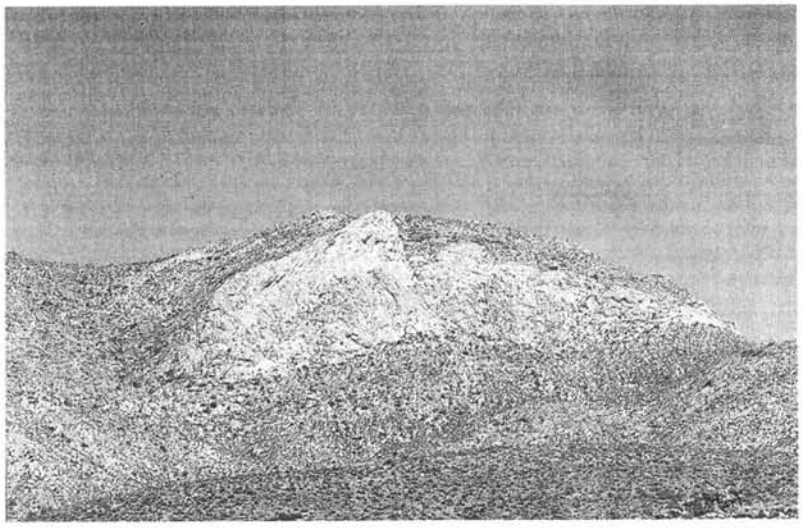

Fig. 4. View from Secret Pass of the west slope of Meiklejohn Peak with the Ordovician (Lower Whiterock Series) lime mud-mound. Even though beds dip steeply into the mountainside, this view highlights the whaleback or dolphin-back geometry of the mound. Note that the mound is asymmetrical, elongate and wedge-shaped and has light grey limestone aprons extending for several hundred metres to the north and south.

grew and evolved from a ramp into a shelf (Ross et al., 1989). However, the ramp stage lasted only briefly during the Early Middle Ordovician (Early Whiterockian). The mound also grew at this time in an outer ramp environment, many tens to hundreds of kilometres offshore, and below storm wave-base (Ross et al., 1989; Sprinkle and Guensberg, 1995; Krause, 1999, 2000). Evidence in support of this interpretation is based not only on the location of the mound relative to its carbonate platform, but also on the regional distribution of lithofacies. Significantly, coeval middle ramp deposits to the east, in eastern Nevada and western Utah, accumulated in shallow water, above storm wave-base. These deposits are interbedded with storm-reworked conglomerates and cross-bedded, skeletal grainstone (Ross et al., 1989; Sprinkle and Guensberg, 1995). On the seaward side of the middle ramp, calathid algae, receptaculitid and sponge-bearing buildups, interbedded with calcareous and terrigenous siltstones, are common (Johns, 1995). These deposits appear to have accumulated at variable depths, near or above storm wave-base, and well within the photic zone (Ross et al., 1989; Johns, 1995; Sprinkle and Guensberg, 1995). On the other hand, the Lower Ordovician (Ibexian or Tremadocian to Middle Arenigian) deposits of the Nine Mile Formation, underlying the mound, and laterally equivalent rocks of the Vinini Formation of central Nevada, represent an older, deeper water, clastic wedge. These terrigenous deposits accumulated near or well below storm wave-base and may represent rocks that were laid down in even deeper water as lowstand wedge submarine fans (Finney and Ethington, 1995; Sprinkle and Guensberg, 1995). Characteristics of similar and equivalent formations in the vicinity of the Meiklejohn Peak mud-mound are highlighted in Table 1.

2.2. Mud-mound stratigraphy, sedimentation and geometry

2.2.1. Mud-mound perimeter

As viewed from inside Secret Pass, the mud-mound is a light grey, asymmetrical, dome with light grey aprons that taper and extend for several hundred metres at either end to the north and south (Fig. 4) (Ross and Cornwall, 1961; Krause and Rowell, 1975; Ross et al., 1975). The whole structure has the outline of a whaleback or a dolphin's

Table 1
Stratigraphy, lithology and depositional environments for rocks in the immediate vicinity of the Meiklejohn Peak Mud-Mound

Stratigraphy[a]	Lithology/composition	Interpreted depositional environment
Goodwin Limestone	Dolomitic limestone, resistant, grey, thin to medium bedded, bioturbated, echinoderm and trilobite bioclasts dominant, lesser ooids, oncolites and peloids, intraclastic, amalgamated calciturbidites and calcidebrites.	Periplatform and slope derived sediment, heterozoan and photozoan bioclasts, sediment gravity flow deposits, cool–cold water, outer ramp.
Nine Mile Formation	Terrigenous siltstone and dolomitic marlstone, recessive, yellow-brown, very thin to medium bedded, grey limestone nodules, current rippled, ooids, oncolites, echinoderm and trilobite bioclasts, *Chondrites isp.*, mineralized erosion surfaces.	Periplatform and slope derived terrigenous sediment, lower flow regime current bedding, heterozoan and photozoan bioclasts, accumulation below storm wave base, outer ramp.
Lower Antelope Valley Limestone	Mud-mound limestone, light grey resistant, thin to medium bedded, flanks current bedded echinodermal grainstone and packstone, core with sparry stromatactis and zebra mudstone and wackestone, pebble-boulder breccias, slumps, neptunian and injection dykes. Intermound dolomitic limestone, dark grey and yellow, resistant, thin to medium bedded, nodular, mudstone, bioclastic wackestone and packstone, current bedded echinodermal grainstone.	Heterozoan bioclasts dominant, abundant early submarine spar and mudstone cementation, zebra and stromatactis cavities, sediment gravity flow deposits, subcutaneous slumps and breccias, submarine vents, frost heave structures after gas clathrate hydrates, accumulation below storm wave-base, photic zone and thermocline, cold–cool water, outer ramp.

[a] Table based on this study, Ross et al. (1975, 1989), Ross and Ethington (1991), Sprinkle and Guensberg (1995), Krause (1999, 2000).

back. In extent this dome is 80 m high north of its centre and stretches out along a variably interdigitating, but generally flat base for approximately 320 m. Next to the mound, the wedges are approximately 30–40 m thick, but they thin to approximately 20 m a few hundreds of metres away. Limestone beds in these wedges comprise predominantly light grey, echinodermal limegrainstone and limepackstone. The mound is underlain and overlain by darker coloured, typically nodular limestone.

Along the base of the mound, dark to medium grey, nodular mudstone to packstone of the lowermost Antelope Valley Limestone is replaced by light grey, mud-mound mudstone and wackestone abruptly, or gradually. Where the lithologic transition is abrupt, the change occurs across a short span typically 1.5 m thick. On the other hand, where the lithologic transition is gradual this change occurs over a 5-m span and intertonguing with light grey mud-mound limestone and dark grey, nodular, fossiliferous mudstone, wackestone and packstone is common. Similarly, along the top boundary of the mound, the lithological change between mound and cover deposits is as varied as that along the base. At some locations, the top contact is sharp and erosional, but at others it intertongues. The intertonguing is very complex, as multiple lenses of light and dark grey limestone may occur along a single layer. The impression that is gained is that simultaneous and multiple centres of mound growth were developing at once. Thus, the top perimeter of the mound appears to have had an intricate depositional history that included periods where parts of the mound were exposed subaqueously, and others where growth was associated with variably thick sediment cover.

As highlighted at the beginning of this section, the general outline of the top of the mound in distant views is that of a whaleback or dolphin's back dome. However, close-up examination indicates that this outline is far more complex, as the dolphin's back is marked by bumps and saddles of variable height (Fig. 4). Two large bumps are readily apparent near the centre of the mound (Fig. 4). Southwards, away from the second bump, the top of the mound is corrugated and intertonguing with overlying beds is common. On the other hand, north and away from the central northern bump, the outline is smooth and the contact with overlying beds is sharp. Here, the top of the mound has an initial and gradual slope of 15–20°, but approximately two thirds of the distance from the northern bump the slope changes abruptly and becomes steeper, reaching approximately 55° (Fig. 5). As shown in more detail in the subsequent section, this slope may have been steeper, but this relationship has been obscured by subcutaneous failure of this end of the mound. Nonetheless, particularly where the slope is less steep, the contact between the mound and overlying beds is sharp and overlying beds onlap. The stratigraphic relationships between the mound and covering beds along this end of the dome indicate that the mound was exposed and that it had topographic relief above the surrounding seafloor at the time of deposition. The mound may have projected above the surrounding seafloor by as little as 15–20 m and by as much as 30 m. Thus, at the time of deposition, along the top, the mound would have been partially exposed to the north, would have been partially covered by sediment to the south, and the whole structure would have projected several metres to tens of metres above the surrounding seafloor.

2.2.2. Mud-mound south end and interior

The internal geometry of the mud-mound is also suggestive of an intricate growth history, as layering can be seen to have different orientations. Layers can be horizontal, or they can dip both to the south and to the north. On the southern half of the mound, both south and northward dipping layers can be seen to intersect (Fig. 6). Here, southward dipping layers downlap and overstep northward dipping layers. In this area the mound is characterized by having inclined echinodermal grainstone and packstone beds that have a northward slope with apparent dips of 10° (Fig. 6). They are intersected and covered by southward dipping mud-mound mudstone and wackestone layers that have apparent dips as high as 20° (Fig. 6). The underlying echinodermal beds form large, metre to decametre size, cross-beds that are further arranged in cosets separated by erosional surfaces of variable lateral extent (Fig. 6).

Echinodermal beds would represent a stage of sediment accumulation that preceded major mound development. At this time, echinoderms would have become established on the seafloor in extensive thickets, indicated by the superabundance of echinodermal particles. Echinoderms became established well away

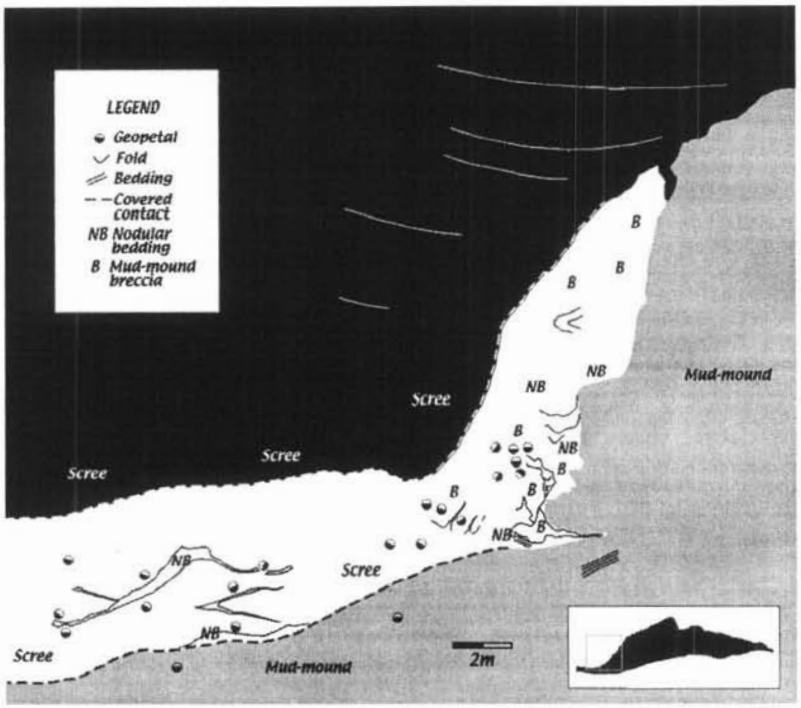

Fig. 5. Map of the northern margin of the Meiklejohn Peak mud-mound illustrating vertical fracture and deformed zone with brecciated mud-mound limestone, slumped nodular layers and covering beds. Scale is approximate as the photograph base used for mapping was not corrected for perspective distortion.

from the area that eventually became the main site of mud-mound development. This behaviour has been noted in the Straits of Florida where stalked crinoids in water depths greater than 600 m are common on soft sediment between hard ground pavements and lithoherms (Neumann et al., 1977). Further, the super-abundance of echinodermal particles on the south flank of the mound is indicative of particle transport

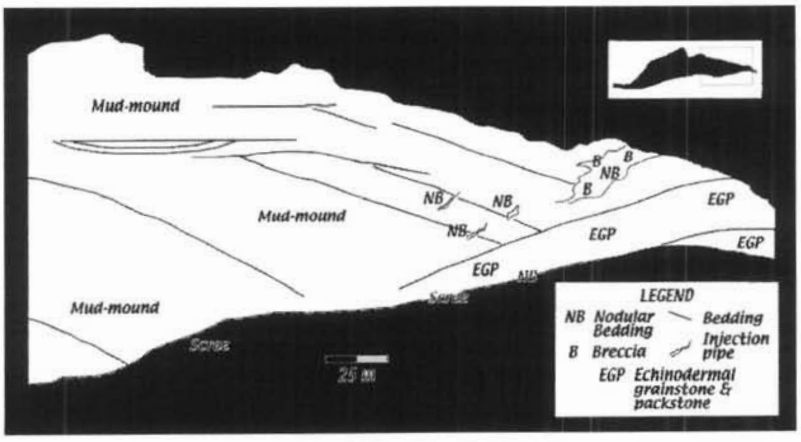

Fig. 6. Map of the southern margin of the Meiklejohn Peak mud-mound displaying internal layering and location of injection dykes and breccia pipe of a submarine vent. Scale is approximate as the photograph base used for mapping was not corrected for perspective distortion.

from nearby sources, as beds higher on the ramp are characterized by ooids, oncolites, sponges and algae (Ross et al., 1989; Johns, 1995; Sprinkle and Guensberg, 1995). Following death and decay, echinoderm derived particles would have been entrained by currents capable of transporting at least coarse sand to small pebble size particles. As indicated by the large-scale cross-bedding, echinoderm particles accumulated in a large submarine dune that rose several metres above the surrounding seafloor. That this condition is not unusual is indicated by large carbonate sediment drifts in water depths exceeding 800 m that include granule to mud-sized materials that have been described from the Northern Straits of Florida (Mullins et al., 1980). These large sediment drifts can be hundreds of metres in size and were stabilized early in their history by submarine cementation. At the Meiklejohn Peak mud-mound, the transport and entrainment of echinodermal particles by currents and accumulation of these particles into a dune may have introduced conditions that facilitated growth of the mound downcurrent. In this scenario, the dune may have provided a leeward shelter that would have permitted the accumulation of carbonate muds and silts, materials which would otherwise have been swept further downcurrent. In addition, as highlighted in a subsequent section, active early submarine cementation would have stabilized mud- and silt-sized materials, and would have also provided very fine-grained cement. This depositional and diagenetic response has been noted in the consolidation of carbonate materials in large sediment drifts and lithoherms at the bottom of the Straits of Florida (Neumann et al., 1977; Mullins et al., 1980).

Mud-mound sediments at Meiklejohn Peak accreted by progressive upward and outward accumulation from as yet an undetermined area near the centre of the mound. As is readily apparent in the southern half of the mound, southward dipping, horizontal, and lenticular layers are common across the area (Fig. 6). This type of layering has also been noted previously in other mud-mounds in the rock record (e.g., Lees, 1964; Wendt et al., 1997; Wendt and Kaufmann, 1998). In addition in the Meiklejohn Peak mud mound, in various places, inclined layers are also truncated erosionally. Thus, muds not only were deposited by progressive upward and outward accretion of sediments, but they were also periodically eroded and presumably redeposited elsewhere. However, truncation of layers at Meiklejohn Peak indicates that erosion only partially removed sediments. Limited erosion may be a result of the strong currents needed to entrain fine-sized sediment once deposited, or muds were stabilized early in the history of the mound. While consolidation is typically attributed to early submarine cementation, muds at the Meiklejohn Peak mud-mound may also have been stabilized by advancing frost fronts as a result of gas hydrate consolidation (as discussed in a subsequent section). Nonetheless, the evidence for early submarine cementation of mudstones and wackestones is common, as neptunian dykes often split these rocks and injection fissures crosscut them (Fig. 6). Neptunian dykes are arranged in simple, complex and crosscutting fissure networks that are cemented with multiple layers of botryoidal to bladed spar. Moreover, the injection dykes and pipes observed at Meiklejohn Peak indicate that mound limestone in places became unstable as zones of overpressure developed. In these zones, overpressured and fluidized, unconsolidated, or partially consolidated sediments were mobilized and injected along fissures that cut across consolidated layers. The largest injection pipe observed, in the southern end of the mound, is nearly 25 m long and is filled with light grey, mud-mound breccia clasts and dark grey, nodular limestone (Fig. 6). This pipe breached the mound, reaching the surface opening onto the surrounding seafloor, and may have served as vent for exiting fluids and fluidized sediments. Thus, injection pipes and neptunian dykes provide evidence that deposits at the mound existed in various states, that ranging from lithified to unconsolidated.

2.2.3. Mud-mound north end and interior

In contrast to the south end of the mound, the north end is typified by having a steep perimeter and bedding with depositional slopes that have apparent dips exceeding 20° and reaching possibly 55°. However, the north end is also characterized by having an extensive zone with large breccia clasts and disturbed bedding between the mound and the nodular limestone beds that overly it (Fig. 5). Mapping of this zone indicates that the main body of the mound is detached from the zone of disturbed bedding by an almost vertical fracture that is approximately 14 m high (Fig. 5). At the top of the vertical fracture is a v-shaped notch that is filled with nodular limestone

similar to the beds covering the mound. The nodular limestone in this notch is tightly folded with the fold axis pointing downwards. The vertical fracture that meets the v-shaped notch continues downwards until it disappears at the bottom in a horizontal v-shaped notch that is also filled with disordered nodular limestone (Fig. 5). Between these two notches the fracture has a variable outline; in its top half it is relatively smooth, but becomes irregular towards its bottom half where it has two small steps before turning 90° into the horizontal v-shaped notch at its base. This horizontal notch may mark a detachment zone within the mound and along which a large block of mound limestone slipped northward.

Fronting the vertical fracture is the zone of brecciated clasts and disturbed nodular bedding. This zone is characterized by having a mixture of light grey, angular clasts of mud-mound limestone with zebra and stromatactis structures and beds with dark grey, folded, oblong, limestone nodules (Fig. 7a). Adjacent to the bottom half of the vertical fracture, beds of nodular limestone are folded into a steep drag fold with fold axes pointing downwards and towards the mound. Underlying this interval of nodular limestone is a breccia zone of light grey mud-mound clasts with very well developed zebra structures. Clasts range in size from small pebbles to boulders that exceed 2 m. Material between the clasts is yellow dolomitic marl with irregular laminae resulting from flowage and sliding. Immediately below the breccia zone is another horizon with tightly folded nodular limestone, steeply dipping bedding that is overturned next to the mound and fold axes pointing downwards.

Throughout this northern zone of disturbed bedding, breccia clasts are variably oriented as can be determined from geopetal fabrics in zebra and stromatactis structures. Close to the mound, clasts have multiple orientations that include steeply tilted and overturned blocks. However, approximately 14 m away from the vertical fracture, brecciated limestone clasts dip at shallower angles and many clasts verge towards the mound. Here interbedded nodular limestone is also broadly folded and several wedge shaped fractures are subhorizontal (Fig. 5). The zone of disturbed bedding and brecciation extends horizontally approximately 35 m before ending in a nose with upturned bedding. Details of the top and bottom contacts of the horizontal zone of disturbed bedding are obscured by scree (Fig. 5).

The stratigraphic relationships noted for the north end of the mound highlight a zone that appears to have formed during the early burial history of the mound, when a significant portion of the mud-mound had already lithified and cover beds had already blanketed the steepest portion of the mound. Brecciation of mound materials indicates that these materials were cemented, and that the zebra and stromatactis structures within were also lithified. Thus, the zone of disturbed bedding and brecciated clasts represents an area along which at least a partially lithified section of the mound became unstable and collapsed. Evidence for collapse and slumping is present in the steeply dipping drag folds with downward pointing fold axes that are common in nodular-bedded deposits next to the mound. Collapse of the mound is also indicated at the vertical notched fracture that is filled with tightly folded nodular limestone with a downward pointing fold axis. Here beds covering the mound were extruded into the notch as it opened. If the notch had been open prior to the deposition of the covering beds, these beds would onlap the walls. Further, slumping also appears to be indicated in the horizontal extension of the zone of disturbed bedding that is several metres away from the mound, as in this area large clasts are upright and many verge gently towards the mound. Nodular beds between these large clasts are folded broadly. The impression gained is that this zone was pushed, broken and folded by the material that collapsed next to the mound. Additional evidence that covering beds had accumulated and filled at least to the steepest edge of the mound is indicated by beds that dip towards the mound and that next to the mound are also broadly folded and rotated downwards (Fig. 5). Lastly, covering beds approximately 20 m above the uppermost notch are essentially horizontal and onlap the mound. Thus, all these features are indicative of

Fig. 7. Meiklejohn Peak slump and breccias. (a) Breccia bed and slump on the north flank of the mound. Zebra and stromatactis limestone clasts are overlain by folded, but nodularly interbedded packstone to mudstone. Hammer handle has a 150-mm scale. (b) Close-up of breccia with pebble- to boulder-sized angular blocks. Note spar cemented zebra limestone blocks. Bar scale towards bottom left is 3 cm long. (c) Drag-folded nodularly interbedded limestone below breccia in panel (a). Hammer for scale. Hammer handle is ~30 cm long.

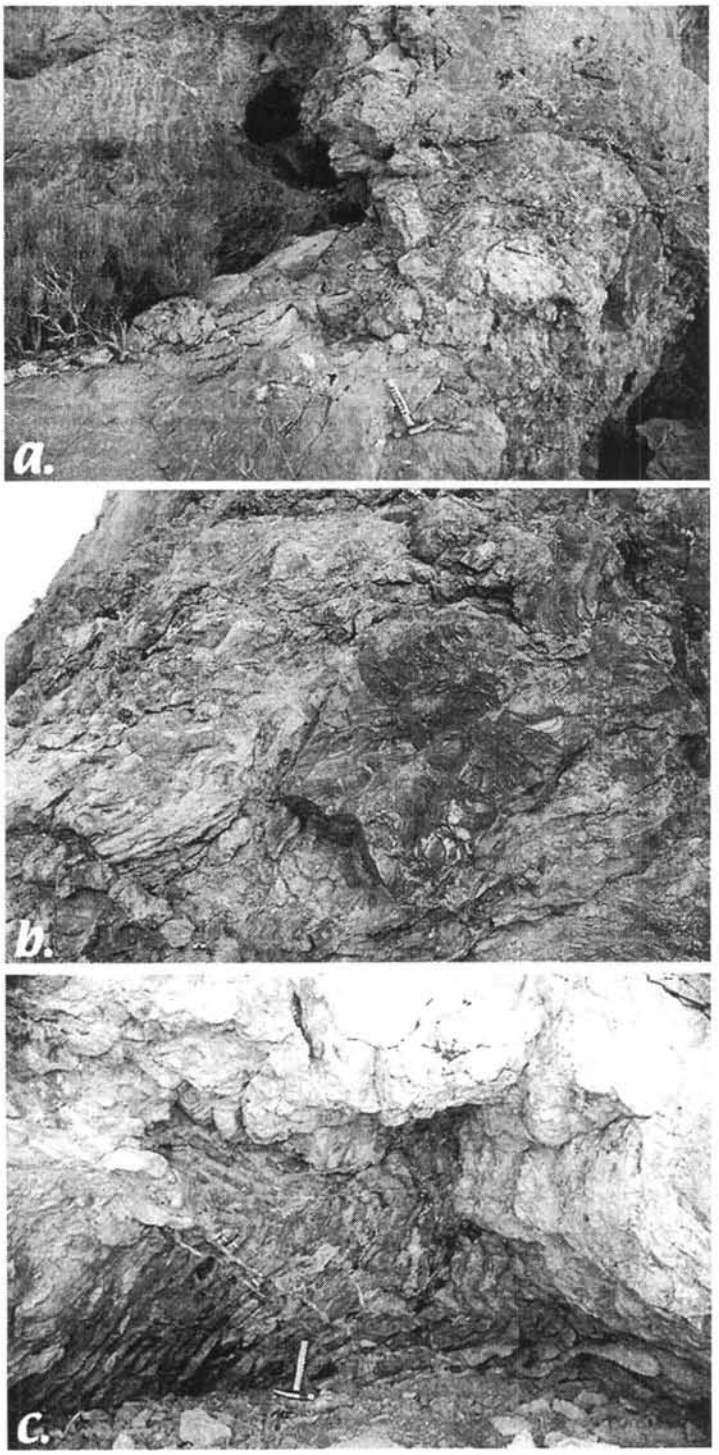
a.
b.
c.

subcutaneous slumping and collapse of this northern section of the mound early in its burial history.

3. Zebra and stromatactis structures: cavities of unknown origin

3.1. Zebra and stromatactis structures

The Meiklejohn Peak mud-mound limestone is characterized by abundant zebra and stromatactis structures. Stromatactis limestone structures have been known for 120 years since Dupont (1881) first identified them. As presently defined, stromatactis typifies mudstone and wackestone with reticulate and swarming masses of cavity-filling spar that have smooth bottoms and digitate roofs (Bathurst, 1982). On the other hand, zebra limestone characterizes laterally extensive and relatively uniform, layered, spar-filled cavities that alternate with mudstone and wackestone bands (Bathurst, 1982). Spar bands overlie mudstone floors where depressions are often filled with layered, commonly peloidal, mudstone. This depositional pattern frequently gives the base of the spar band a smoother bottom than the top. Thus, spar bands are infilling parallel cavities where the perimeter of the floor and the ceiling may sometimes match.

3.2. Previous work and interpretations

Zebra and stromatactis limestone structures have been a source of enduring geological interest ever since Dupont (1881) first noted them. A range of explanations have been favored: decay of soft-bodied organisms, plants and cyanobacterial mats (Bathurst, 1959; Philcox, 1963; Lees, 1964; Wolf, 1965; Ross et al., 1975; Pratt, 1982; Bourque and Gignac, 1983; Bourque and Boulvain, 1993; Reitner et al., 1995; Kaufmann, 1998); sheltering and baffling by a skeletal or soft-bodied framework (Schwarzacher, 1961; Lees, 1964; Lees and Miller, 1995); recrystallization of former skeletons and mud (Black, 1952; Orme and Brown, 1963; Ross et al., 1975); microbialites (Lees and Miller, 1995; Monty, 1995; Pratt, 1995; Reitner et al., 1995; Kaufmann, 1998); openings created by roots and burrowers (Bechstädt, 1974; Shinn, 1968); recrystallization of carbonate mud and dissolution during low-grade metamorphism and pressure dissolution (Logan and Semeniuk, 1976); precipitation of mud and spar from hydrothermally vented fluids (Mounji et al., 1998); dilatation of carbonate mud from shear failure downslope (Schwarzacher, 1961); and channelways associated with non-uniform sediment compaction and dewatering (Heckel, 1972; Lees and Miller, 1995; Wendt et al.,1997; Wendt and Kaufmann, 1998). A common thread linking these explanations was championed by Bathurst (1959, 1977, 1980, 1982), who suggested that stromatactis and zebra fabrics reflected ramifying and labyrinthine cavity systems infilled with spar.

3.3. Early cavities and cemented crusts

Zebra and stromatactis limestone share a common origin as was elegantly shown by Bathurst (1982) in Paleozoic mud-mounds. He noted clearly that stromatactis and zebra limestone structures were cemented carbonate crusts and cavities stabilized by early submarine lithification of carbonate sediment (Bathurst, 1977, 1980). These ideas significantly expanded knowledge about these structures and rock types. Nonetheless, the underlying geologic agent or process, which imprinted Precambrian and Phanerozoic rocks with these cavity systems, has continued to elude identification.

3.4. Cavities and cavity systems of unknown origin

Although many researchers studying zebra and stromatactis fabrics in Phanerozoic mud-mounds have favoured an organic origin, perhaps by softbodied multicellular organisms leaving a cavity upon decay, the responsible geological agent was also common in the Precambrian, prior to the advent of organisms with abundant mineralized skeletons in the Earliest Phanerozoic (Tucker, 1983; Pratt, 1995). This latest observation lends credence to the notion that these fabrics, while still organic, are somehow microbial constructs (Monty, 1995; Pratt, 1982; Kaufmann, 1998). However, the answer may lie in between, as these structures may represent physically modified sediment to which microbes contributed their metabolic byproducts. Evidence presented below advances the concept that these limestones preserve imprintings that are the product of heaving and early submarine cementation, responses to synsedimentary cryotur-

bation during consolidation and dissociation of gas clahtrate hydrates (gas-charged ice) and simultaneous incongruent precipitation of carbonate cements.

4. Gas-charged ice, carbonate cementation and $\delta^{13}C-\delta^{18}O$ stable isotopes

Growth and development of gas clathrate hydrates is independent of geologic age, as they are crystalline compounds that form when water with dissolved gases rearranges itself and freezes at the right temperature and pressure into a solid, porous, and often permeable phase. Under these conditions, water molecules form cage-like structures that may typically contain gas or gas mixtures. Interestingly, clathrate hydrates may be surrounded by gas, liquid and water, and may contribute to the precipitation of mineral phases in enclosing sediments, such as calcite, aragonite, siderite and/or dolomite (e.g., Sakai et al., 1990; Roberts et al., 1992; Roberts and Carney, 1997; Bohrmann et al., 1998; Booth et al., 1998; Orange et al., 1999). The most common gases entrapped in clathrate hydrates are methane, ethane, propane, carbon dioxide and hydrogen sulphide (Katz et al., 1959; Claypool and Kaplan, 1974; Hitchon, 1974; Sakai et al., 1990; Roberts et al., 1992; Kvenvolden, 1998; Sassen et al., 1998; Sloan, 1998a,b). In modern ocean basins, methane clathrate (C1 hydrocarbon) is the most common hydrocarbon clathrate hydrate variety observed to date, as it solidifies at progressively higher temperature with increasing pressure (Fig. 8) (Katz et al., 1959). It is often found in the ocean at pressures greater than 5–7 MPa and at temperatures below 7.5 °C (Claypool and Kaplan, 1974; Roberts et al., 1992; Bohrmann et al., 1998; Booth et al., 1998; Orange et al., 1999). On average, at low and mid-latitudes under the thermocline, temperatures lower than 7.5 °C are common below a depth of 1 km and, at much shallower depths, in zones of upwelling (Thurman, 1988). In this environment methane clathrates would be stable at depths as low as 300 m if water temperatures were near 0 °C (Fig. 8) (Katz et al., 1959; Hitchon, 1974; Kvenvolden, 1998; Sloan, 1998a). On the other hand, at these conditions carbon dioxide clathrate hydrates would be stable at even shallower depths, 140 m or even slightly less (Fig. 8) (Katz et al., 1959; Miller, 1974; Sakai et al., 1990).

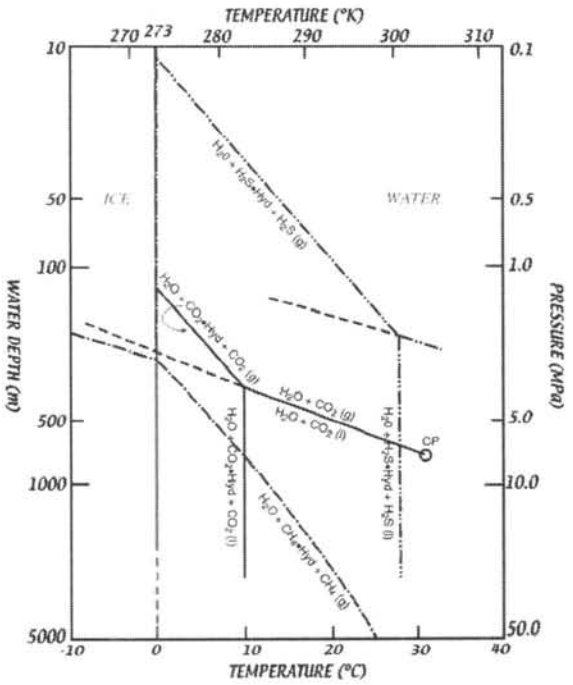

Fig. 8. Pressure, temperature and depth phase diagram for CH_4, CO_2 and H_2S in pure water (diagram based on the data from Katz et al., 1959 and Miller, 1974). In seawater, the gas clathrate hydrate phase boundary of a pure phase shifts slightly to the left, but addition of a small amount of another molecule, for example of H_2S to both CO_2 and CH_4, shifts this boundary towards the right. This latter condition is typical in oceanic settings as gases are commonly mixed. Grey line at 273 °K (0 °C) highlights the ice and water phase boundary.

Methane, the most common gas in modern marine environments, is derived principally from two sources: the active anaerobic decomposition of carbon dioxide and organic substances by methanogenic bacteria in seafloor sediments; or from gases associated with hydrocarbon seeps (Claypool and Kvenvolden, 1983; Roberts et al., 1992; Kvenvolden, 1998). A number of methanogenic bacterial reactions are known, typically yielding methane (CH_4), carbon dioxide (CO_2), bicarbonate (HCO_3^-), water (H_2O) and other byproducts (Claypool and Kaplan, 1974; Brock and Madigan, 1991). Moreover, in close proximity to the seafloor and in the absence of significant amounts of biogenic CO_2 production, interstitial methane generation tends to raise pH and favour carbonate precipitation and cementation of surrounding sediment (Claypool and Kaplan, 1974; Bohrmann et al., 1998; Orange et al.,

1999). Carbonate minerals precipitated in this fashion may follow the pathways originally proposed by Claypool and Kaplan (1974) where interstitial fluid alkalinity and chlorinity increase with clathrate hydrate consolidation (Harrison et al., 1979; Jenden and Gieskes, 1980; Hesse, 1990).

One well-documented instance of a clathrate hydrate composed predominantly of carbon dioxide (86–92% CO_2, 3–5% H_2S, and 3.5–11% CH_4 and He) has been reported from offshore Japan at depths of 1300–1550 m in the mid-Okinawa Trough Backarc Basin (Sakai et al., 1990). Here, at the sediment–water interface, CO_2-rich liquid has been observed issuing from volcaniclastic sediment and consolidating as it comes in to contact with overlying seawater. This response matches the known phase behaviour for CO_2 and water at this depth and temperature (Fig. 8) (Katz et al., 1959; Miller, 1974). Sakai et al. (1990) indicate further that sediment below the seafloor is very likely indurated with carbon dioxide hydrate. In this context, identification of carbon dioxide hydrate in the seafloor is important, as it may be an excellent sedimentary paleothermometer. Phase relationships for carbon dioxide in pure water indicate that the clathrate hydrate consolidates when the isotherm remains below 10 °C and water depth is below ~360 m (Fig. 8). Carbon dioxide clathrate hydrate is also stable at shallower depths, but under these conditions requires temperatures lower than 10 °C and can theoretically consolidate at ~140 m water depth at 0 °C (Fig. 8).

Analyses of stable isotopes of calcite from Meiklejohn Peak zebra and stromatactis structures yielded ratios between 1‰ to −1‰ $\delta^{13}C$ and −6‰ to −11‰ $\delta^{18}O$ (Fig. 9). This data is consistent with isotopic ratios of carbonates precipitated from Ordovician seawater and that have a range between −2‰ to 6‰ $\delta^{13}C$ and −0.5‰ to −10.5‰ $\delta^{18}O$ (Tobin and Walker, 1995; Veizer et al., 1997; Carpenter and Lohmann, 1997). The $\delta^{13}C$ values from the mud-mound are significantly higher than those recorded from carbonates derived from the oxidation of methane which typically range between −55‰ and −20‰ (Beauchamp and Savard, 1992; Aharon et al., 1997; Roberts et al., 1992; Roberts and Carney, 1997; Bohrmann et al., 1998; Orange et al., 1999). However, the $\delta^{13}C$ isotopic ratios are close to isotopic ratios obtained for seafloor ΣCO_2

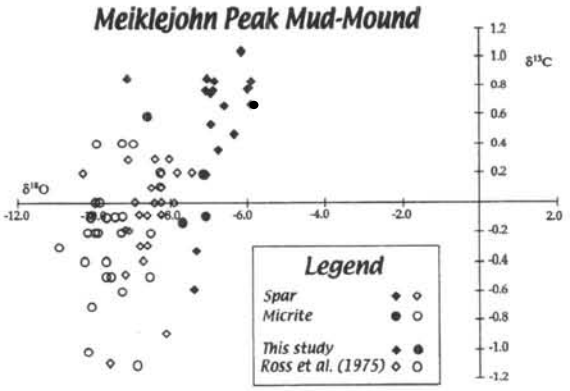

Fig. 9. Cross-plot for $\delta^{13}C$ and $\delta^{18}O$ PDB isotope ratios for micrite and spar from zebra and stromatactis limestone from the Meikejohn Peak mud-mound. Open circles and diamonds highlight carbon and oxygen isotope data published previously by Ross et al. (1975). Original $\delta^{18}O$ SMOW scale data of Ross et al. (1975) has been recalculated to the PDB standard scale using the method of Friedman and O'Neil (1977). Two of the converted compositions of sparry cement reported by Ross et al. (1975) fall outside the main area of the plot and have not been included with this diagram. These cements have $\delta^{13}C$ and $\delta^{18}O$ isotopic ratios that are −0.1‰ and −1.8‰, and −51.7‰ and −16.7‰, respectively. The $\delta^{18}O$ isotopic ratio from the first of these two samples is extremely low and very likely reflects a late stage cement from a crosscutting calcite veinlet that is associated with tectonism and mountain building.

(Claypool and Kaplan, 1974; Sakai et al., 1990). Thus, the data may indicate that frost heave structures from the mound are instead the product of carbon dioxide clathrate hydrates.

In deep water, below the photic zone and outward of the shelf edge, interstitial fluids saturated with CO_2 may exist in areas of abundant carbonate sediment accumulation. Conditions such as those proposed here have been identified in terrigenous slope sediments of Southern California in 800- to 1200-m deep water (Presley and Kaplan, 1968). At this locality, saturation gradients with respect to calcium carbonate are present in the sediment column below the seafloor. The first 2 m of the sediment column are undersaturated, most likely from the release of metabolic carbon dioxide. However, below 2–3 m the sediment becomes supersaturated with respect to calcium carbonate (Presley and Kaplan, 1968). Thus, in this type of environment CO_2-rich fluids may consolidate interstially at appropriate temperature and pressure, leading to the formation of CO_2 cloth-

rate hydrates. This process may also be an important mechanism for early calcium carbonate precipitation, as appreciated from fundamental carbonate equilibria (Bathurst, 1971). Significantly, as the CO_2 clathrate hydrate consolidates, removal of CO_2 from surrounding interstitial seawater would result in localized precipitation of $CaCO_3$ and early subseafloor cementation and lithification

$$CO_2 + H_2O + CaCO_3 \rightleftarrows Ca^{2+} + 2HCO_3^-$$

Thus, carbon dioxide clathrate hydrate could consolidate very near the seafloor, leaving structures in the sediment column that may be stabilized by early submarine cementation.

5. Zebra and stromatactis structures and cryoturbic textures

Zebra and stromatactis limestone structures are thought to be synsedimentary submarine cavity systems that were stabilized by early submarine cementation (Bathurst, 1977, 1982). Past explanations for these structures have included the following: decay of soft-bodied organisms, plants and cyanobacterial mats; sheltering and baffling by a skeletal or soft-bodied framework; recrystallization of former skeletons and mud; microbialites; openings created by roots and burrowers; recrystallization of carbonate mud and dissolution during low-grade metamorphism and pressure dissolution; precipitation of mud and spar from hydrothermally vented fluids; dilatation of carbonate mud from shear failure downslope; and channelways associated with non-uniform sediment compaction and dewatering (as per references cited on p. 224). However, these explanations fail to account for previously discussed sedimentological characteristics observed at the Meiklejohn Peak mud-mound. In particular, they do not explain how these openings were supported and kept open prior to stabilization by early cementation? (e.g., Ross et al., 1975). This question is reinforced when considering zebra limestone sheet cracks, as these openings are known to extend for distances that are tens to hundreds of times greater than their width, with cavities having extensive micrite floors and ceilings (e.g., Lees, 1964; Ross et al., 1975; Bathurst, 1980, 1982). The premise proposed here is that at the Meiklejohn Peak mud-mound cavities were propped up by gas clathrate hydrates (i.e., gas-charged ice). The existence of gas clathrate hydrates in modern oceans is well established; estimated volumes for methane clathrate hydrate alone are vast and are thought to approach 10^{15} to 10^{16} m^3 (350,000 tcf) (Kvenvolden, 1998). If these materials are so common today, then why could they not equally have been common in the past? It is obvious that the preservation of gas clathrate hydrates far back in geologic time is unlikely, but evidence for their former growth and consolidation should exist. Perhaps cryoturbic structures and textures, which are well known for standard ice, may also be common to gas clathrate hydrates.

Cryoturbation textures and structures are preserved when water and ground freeze and thaw seasonally, and a number of them have been identified in studies of frozen sediment on land (Taber, 1929, 1930; Beskow, 1935; Romans et al., 1980). The preservation of cryoturbic fabrics should be expected particularly where conditions for early carbonate cement precipitation accompany gas clathrate hydrate formation. Known occurrences of methane clathrate hydrates in cores and grab samples from modern seafloors indicate that the sediments at the time of collection and prior to dissociation are, at least, partly consolidated (Harrison et al., 1979; Malone, 1990; Roberts et al., 1992; MacDonald et al., 1994; Suess et al., 1999). In these sediments methane clathrate hydrates have characteristic growth habits, as they are typically found disseminated in the pore space, or agglomerated as deposits where they are displacive, consolidating into massive, nodular, branching or layered aggregates (Malone, 1990; Ivanov et al., 1998; Sloan, 1998b; Suess et al., 1999). Significantly, the frost heave layering of methane clathrate hydrates originally figured by Malone (1990) resembles that observed in zebra limestone (Figs. 10 and 11a).

5.1. Zebra-like fabrics

In frozen Arctic and alpine ground environments, a common fabric which strongly resembles the zebra limestone sheet cracks from Meiklejohn Peak includes ice layers which accumulate into multiple, stacked, horizontal to vertical lenses and sheets. These ice deposits are known as *segregation ice*.

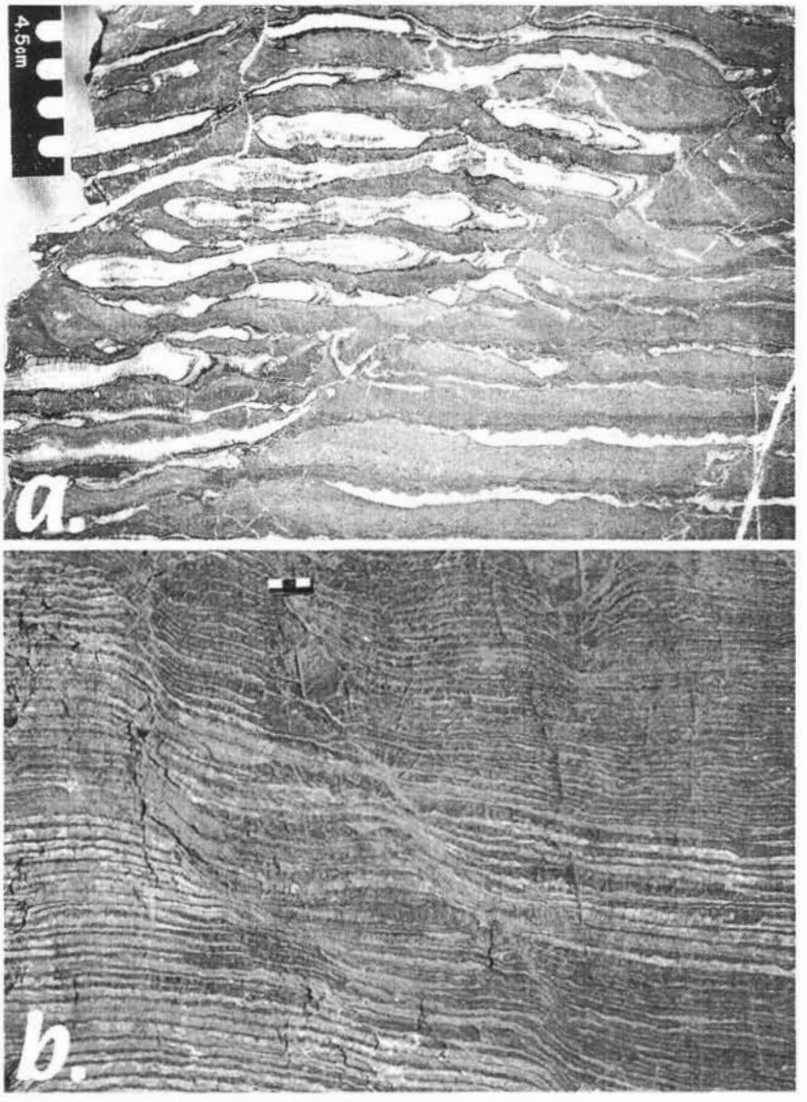

Fig. 10. Zebra limestone with differentially heaved layers. (a) Polished rock cut that displays zebra spar bands, which are variably thick along their lengths. As a group, layers to the left are thicker than layers to the right. Layers to the left are also gently drag-folded and thrust along a diagonal line. This pattern is the result of *differential* heaving and dilatation of parallel fissures below the seafloor. (b) Zebra limestone with parallel and subparallel layering that resembles *segregation ice* sheets and lenses observed on land in permafrost, in laboratory experiments with advancing freezing fronts of water–ice in sediment cores, and in seafloor samples of methane clathrate hydrates (Taber, 1929, 1930; Beskow, 1935; Romans et al., 1980; Malone, 1990; Ginsburg et al., 1993; Suess et al., 1999). Note also that zebra bands form stacks that are separated and highlighted by curving kink bands. These stacks of zebra spar bands may be the product of differential heaving during consolidation, expansion and dissociation of layered gas clathrate hydrates.

The physical deformation process that accompanies the accumulation of segregation ice is *frost heave* (Taber, 1929, 1930). Segregation ice lenses and sheets typically develop in very fine-grained sediments, and less frequently in sand-sized sediment, where they commonly form immediately below overlying layers of finer-grained materials (Taber, 1929, 1930; Beskow, 1935). At Meiklejohn Peak, sheet-cracked zebra limestone typically occurs in the fine-grained mudstone and wackestone of the mud-mound

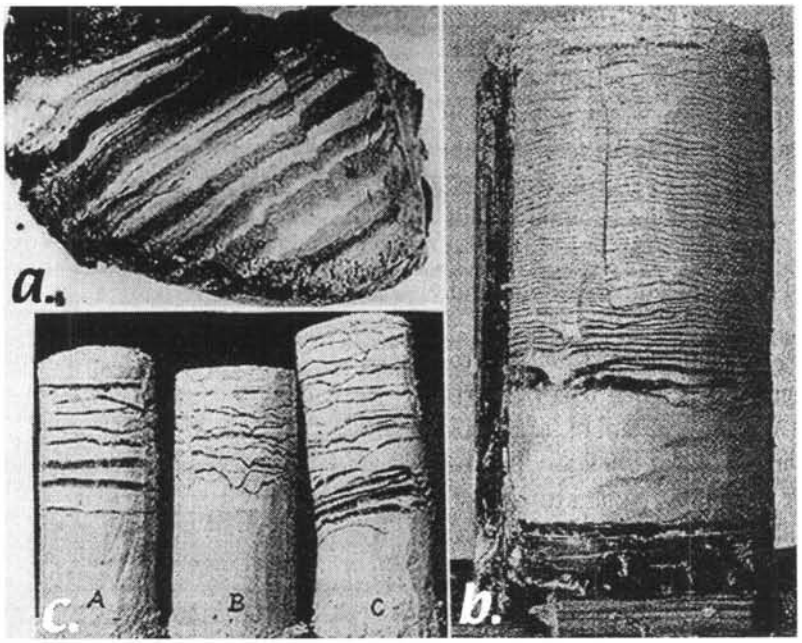

Fig. 11. Seafloor methane clathrate hydrate sample and *segregation ice* frost heaved sediment cores. (a) Core fragment from deep sea drilling in the Blake Plateau area with parallel layered methane clathrate hydrate and frozen seafloor sediment (photo courtesy of R.D. Malone). (b) Core from a laboratory experiment originally illustrated by Taber (1930) that displays parallel ice-filled sheet cracks and bands of frozen sediment. Fissures opened in clay-size sediment and filled with ice (black layers in the photograph) during downward advance of a freezing front. This core was originally weighed down with iron weights to an equivalent load of 0.8 MPa. Core diameter, ~85 mm. (c) Three cores packed with clay-sized sediment displaying ice-filled sheet cracks (from laboratory experiments illustrated by Taber, 1929). Sediment fracturing and ice infilling occurred during progressive downward advance of a freezing front. Core A, unloaded; core B, weighed with 7.4-kg iron weights, but separated by a wood spacer (compressive stress ~15 kPa); core C, weighed directly with 7.4 kg iron weights (compressive stress ~15 kPa). Note that snout-like synforms and socket-like fissures are common in weighed cores. All cores are 78 mm in diameter. Upper case letters are Taber's.

(Fig. 10a and b). In only rare instances are spar-filled sheet cracks observed in the encrinites on the north and south flanks of the mound. In these examples, they occur within or below mudstone and wackestone interbeds.

Segregation ice lenses and sheets were reproduced by Taber (1929, 1930) and Beskow (1935). Both researchers froze water-saturated sediment and noted that clay-sized particles, abundant small voids, a constant supply of water, and freezing fronts with constant rates of cooling had the desired effect of reproducing segregation ice layers (Fig. 11b and c). In his experiments, Taber (1930) also varied the nature of fluids in the sediment. Using benzene and nitrobenzene, two fluids which decrease in volume upon freezing, he obtained segregation ice layers like those that he had observed with water. Taber (1929, 1930) also identified that the rate of cooling was a clear determinant in the rhythmic frequency and spacing of fissures. As the rate of cooling decreased, ice-filled fissures appeared to become larger and the intervening clay layers became thicker. In deposits from modern sea floors, segregation methane clathrate hydrate layers have been illustrated by Malone (1990), Ginsburg et al. (1993) and Suess et al. (1999).

In a series of experiments, Taber (1929, 1930) placed loads of different weight on clay filled cylinders, including weights up to 0.8 MPa. Under these conditions, sheet cracks formed as in the unloaded cores, but in many instances fissures curved downwards, forming concave fractures with a downward protruding clay roof. In cross-sectional view, this clay layer resembles a small muddy synform or cusp (Taber, 1929, 1930) (Fig. 11b and c). These curved

sheet cracks are significant, as they result in a sedimentary structure that preserves heaving. As a freezing front advances downwards, new sheet cracks develop at either side of the concave fissure, intersecting this fissure as they propagate and establishing a cross-cutting relationship. Although the exact cause for curved, downward deflecting fissures with overlying downward projecting cusps is at present unknown, it is important to note that downward projecting mudstone synforms are common in zebra limestone at the Meiklejohn Peak mound (Fig. 12a). Moreover, many of the mudstone synforms from the mound are underlain with thick spar infillings that clearly reflect responses to heaving and dilatation of the original sediment (Fig. 12a–d). They characterize a new sedimentary structure identified here for the first time as *snout and socket structure*. This structure preserves heaving and dilatation and has been stabilized by early carbonate cementation. Snout and socket structures originate during downward advance of a freezing front as it penetrates the sediment column from above. Occasionally, during lateral propagation, a fissure may deflect downwards if it encounters an inhomogeneity. When this occurs, a concave socket is produced with an overlying mudstone snout or synform. Once a snout and socket have formed, and as the frost front continues to advance downward, a new horizontal fracture develops at either side. However, this new fracture terminates in the opening left behind by the socket fracture. The heave and dilatation associated with the new horizontal fracture is added to the space under the snout. Thus, the socket fracture under the snout enlarges opening and growing in proportion to the dilatation of the horizontal frac-

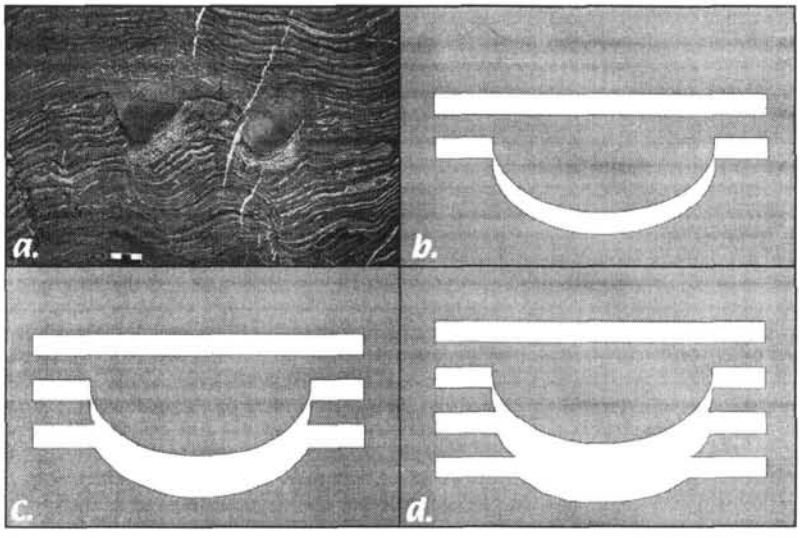

Fig. 12. Snout and socket structure. (a) Zebra limestone with a pair of mudstone synforms underlain by overthickened spar bands. In the Meiklejohn Peak, carbonate mud-mound mudstone synforms like these are common. They appear to be the product of heaving and dilatation in the manner illustrated in the sequential cartoons, panels (b)–(d). Black and white bar scale is 3 cm long. (b) *Cartoon that illustrates the development of a snout-like mudstone synform and a socket-like fissure*. Sediment is intermittently ruptured as a gas clathrate hydrate frost front penetrates and freezes the seafloor. Ruptures propagate laterally growing into segregation clathrate hydrate layers as they are filled with the gas-charged ice. On occasion, instead of propagating evenly, fissures may be forced to deflect downwards by an inhomogeneity. In this case, the rupture is a concave and socket-like opening with an overlying snout-like mudstone synform. (c) *Cartoon illustrating the progressive development of a snout and socket structure following initial rupture*. New parallel fissures develop at either side of the snout as the freezing front continues its downward advance. New fissures extend laterally, but they intersect the socket fracture as they propagate. Significantly, heave associated with these intersecting horizontal fractures is added to the socket fracture below the lines of intersection. Thus, the opening under the snout enlarges in proportion to the amount of heave of the horizontal fracture. (d) *Cartoon illustrating progressive enlargement of the socket fracture at points of intersection under the snout*. Continued advance of the freezing front results in additional fractures that repeat this response, further enlarging the socket fracture below points of intersection. Widening of the opening under the snout by fissuring stops after the freezing front advances and bypasses the socket fracture.

ture (Fig. 12b). Continued advance of the freezing front repeats this process until the freezing front moves beyond and below the socket fracture (Fig. 12b–d).

5.2. Stromatactis-like fabrics

In modern and Pleistocene soils in Iceland and the British Isles, a fabric which bears a striking resemblance to stromatactis, as observed at the Meiklejohn Peak mud-mound, has been identified and named *silt droplet fabric* by Romans et al. (1980, plates 10 and 17). Silt droplet fabric is not restricted to the localities noted above, but has also been identified in alpine environments and in the Canadian Arctic by Bunting and Federoff (1974), Romans and Robertson (1974) and Bunting (1983). Although the exact conditions under which silt droplet fabric develops are not completely known, all these authors agree that silt droplet fabric develops by periodic freezing and thawing of soils. Opening dimensions illustrated for silt droplet cavities by Romans et al. (1980, plate 10) are 2–6 mm in length and 0.1–1 mm in height. These silt droplet cavities are identical to the spar-filled geopetal stromatactis cavities shown, for example, by Bathurst (1982, Fig. 6C), and are similar to some of the smaller stromatactis structures observed at the Meiklejohn Peak mud-mound.

Stromatactis with classical digitate roofs and flat floors, ranging in size from millimetres to decimetres, is common at the Meiklejohn Peak mud-mound (Fig. 13). At some locations, interconnected cavity networks are highlighted by layered, red coloured, geopetal mudstone that stands out in rich contrast against the light grey host mudstone. Where the geopetal mudstone has not completely filled a cavity network, stromatactis spar with irregular and pointed digits infills remaining openings (Fig. 13a). In contrast, at the Meiklejohn Peak mud-mound, geopetal mudstone and stromatactis spar may occur stacked in tiers, as this mudstone may overly one or more generations of spar (Fig. 13b). The stacked or alternating behaviour for geopetal mudstone and spar has been noted previously in other studies (Lees, 1964; Ross et al., 1975). The presence of multiple generations of spar and geopetal mudstone within these cavity systems is important, because it is indicative of fluctuating environmental conditions within these openings. Periods of geopetal mudstone accumulation are separated by stages of spar precipitation in the microenvironment of these cavities. This behaviour may be a response to alternating or reversing conditions where a time of hydrate consolidation was followed by a period of hydrate dissociation. Significantly, the consolidation and dissociation of gas hydrates over time has been observed on the bottom of the Gulf Mexico (MacDonald et al., 1994; Roberts and Carney, 1997; Sassen et al., 1998). These authors have also noted that clathrate hydrate deposits are accompanied by the evolution of fluctuating gas bubble streams. They also noted that, on occasion, fragments of clathrate hydrate and sediment became dislodged from the main deposit and floated into the overlying water column, carried by the buoyant clathrate hydrate. These observations are significant because they illustrate conditions that may lead to geopetal mudstone accumulation during stages of clathrate hydrate dissociation. Once fluids begin to flow in a cavity, fine-grained sediment and early submarine cemented peloidal mudstone could settle as geopetal fill at the bottom of a cavity, or above a layer of precipitated spar. In contrast, spar and micrite cement may precipitate during clathrate hydrate consolidation stages as pore fluids become supersaturated with respect to calcium carbonate. Supersaturation of interstitial pore fluids with calcium carbonate 2–3 m below the seafloor has been documented in the modern sea floor of Southern California, in water depths of 800 and 1200 m (Presley and Kaplan, 1968). Thus, the conditions proposed for stromatactis and zebra limestone structures at the Meiklejohn Peak mud-mound are similar to ones already noted within modern sea floors.

5.3. Synsedimentary fluid expulsion, sediment intrusion and brecciation

Observations from the floor of the Gulf of Mexico indicate that gas clathrate hydrate deposits wax and wane (MacDonald et al., 1994; Roberts and Carney, 1997). They not only consolidate and grow at the appropriate temperature and pressure, but they dissociate and degas at other times as bottom conditions span the hydrate phase envelope (Fig. 8) (MacDonald et al., 1994; Roberts and Carney, 1997; Sloan, 1998a). At Meiklejohn Peak there are mesoscopic features that may be noteworthy if consolidation, dissociation and

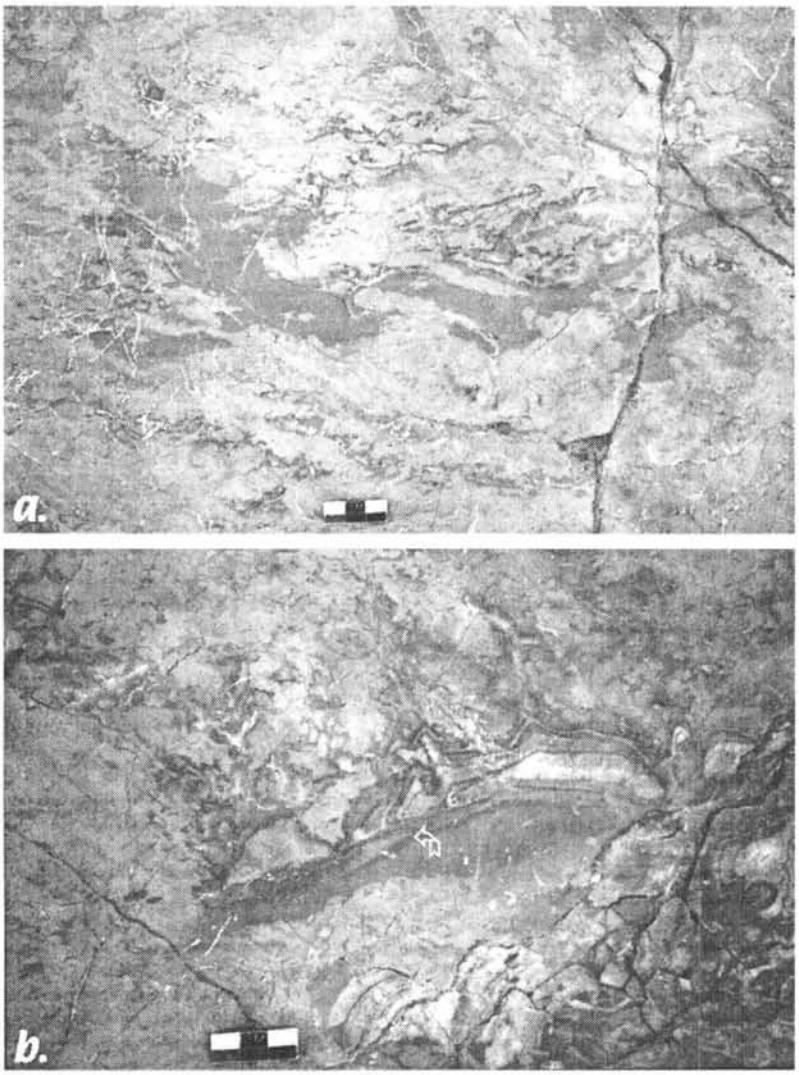

Fig. 13. Meiklejohn Peak stromatactis limestone. (a) Millimetre- to decimetre-sized stromatactis enclosed by light grey limestone and filled with red brown (darker grey in photograph) cavity filling mudstone. Bar scale is 3 cm long. (b) Large stromatactis cavity filled with multiple generations of spar and red brown (darker grey in photograph) geopetal mudstone. Folded white arrow points to a spar layer that overlies laminated mudstone. However, this spar layer is separated from the main and overlying mass of cavity filling spar by a thin layer of laminated geopetal mudstone. Bar scale is 3 cm long.

carbonate cementation, as takes place with methane clathrate hydrates, are considered as a working hypothesis (Figs. 5–8). Sedimentary features that reflect deformation of partially consolidated sediment are common at the Meiklejohn Peak carbonate mud-mound, consisting of fluid expulsion structures, subcutaneous brecciated layers, subcutaneous slumps and slides, breccia filled sills and dykes, folds and thrusts, and possible submarine sedimentary volcanism. All these deformation and injection structures may be a result of synsedimentary gas clathrate hydrate growth and dissociation during the evolution of the Meiklejohn Peak mud-mound.

The most striking sedimentary features are breccia beds with abundant zebra and stromatactis clasts (predominantly pebbles to boulders) and drag-folded

nodular limestone along the northern flank of the mud-mound (Fig. 7). Stratigraphic and sedimentary relationships of these deposits indicate that brecciation and folding occurred as a result of subcutaneous slumping and failure, as described in an earlier section. Failure of materials along this margin may have occurred in response to rapid dissociation of clathrate hydrate, which in turn may have arisen from changing pressure as a result of sea level fall. Similar deformation, but developed to a lesser extent, occurs on the southern end of the mound where a 25-m long breccia pipe reaches the surface of the mound (Fig. 6). This long breccia zone may represent a feeder pipe along which sediment and fluids were expelled, as is the case with sedimentary volcanoes that have been documented with modern hydrate deposits (Roberts and Carney, 1997; Bouriak and Akhmetjanov, 1998; Ivanov et al., 1998).

Breccias with abundant angular clasts of mud-mound strata, including zebra and stromatactis blocks, are indicative of early submarine lithification of these materials and structures (Fig. 7a and b). Nodular limestone clasts that accompany these deposits also appear to have cemented early, as individual nodules are rotated and nodule trains are slumped and folded, and in some instances sheared (Fig. 7a and c). Along the southern flank of the mound, injection dykes and sills with dark grey, lime nodules and yellow dolomitic marlstone matrix have intruded and crosscut light grey mound lime mudstones and wackestones. These fabrics are suggestive of diapirism and fluid expulsion of overpressured sediments and fluids that breached consolidated and lithified materials. Processes like fluid expulsion, diapirism, mud volcanism, and ejection of lithified materials have been reported from a number of modern clathrate hydrate bearing sites (Roberts and Carney, 1997; Bouriak and Akhmetjanov, 1998; Ivanov et al., 1998; Orange et al., 1999). Thus, they should be part and parcel of the preserved sedimentary record when gas clathrate hydrates have intervened in the consolidation history of these rocks.

6. Conclusions

Even though the Meiklejohn Peak mud-mound was a small geologic feature compared to the large ramp on which it grew, its geologic history is significant in the interpretation of marine conditions near and below the Ordovician sea floor at the time of sedimentation. The mound developed in deep, cold water in an outer ramp setting, below the photic zone and well below storm wave base. It was an asymmetrical and elongate submarine feature that had significant relief above the surrounding sea floor. Mound growth commenced near a large submarine dune that was tens of metres in size with northward dipping cross-beds. This dune, composed predominantly of echinodermal particles derived from nearby echinoderm thickets, developed as coarse- to granule-sized particles were entrained by northward flowing currents. In contrast the mound, composed predominantly of lime mudstone and wackestone in horizontal, northward and southward dipping layers, eventually became much higher than the bioclastic dune. Significantly, mud-mound sediments were modified frequently during deposition or shortly thereafter by early, subseafloor processes in response to consolidation and dissociation of gas clathrate hydrates, very possibly carbon dioxide clathrate hydrates.

Cryoturbic modification of mud-mound deposits is indicated by frost heave structures that include *snout and socket*, sheeted cracks and stromatactis structures that formed as frost fronts penetrated the seafloor. Mud-sized and sparry carbonate cements precipitated almost simultaneously with the consolidation gas clathrate hydrates. Early carbonate cement precipitation aided the stabilization of cryoturbic structures through early lithification. Geopetal sediments in zebra and stromatactis structures accumulated within cavities that formed as gas clathrate hydrates dissociated periodically. Internal sediments may have also accumulated with hydrate consolidation, as these materials precipitated at pressures and temperatures where fluids and solids coexisted. Under both situations, localized pressure gradients would have allowed for fluid movement, and transport and precipitation of fine-grained materials in cavity networks below the seafloor.

The Meiklejohn Peak mud-mound strongly resembles the lithoherms identified by Neumann et al. (1977) along the base of Little Bahama Bank in the Straits of Florida. This idea was considered previously by Ross et al. (1975, pp. 45–46), but they stopped short of this conclusion. Correlation of the mound

with lithoherms is based on a variety of common features that include similar elongate morphology, whaleback or dolphin back domes; similar height, as lithoherms rise above the surrounding seafloor as much as 50 m, and early, submarine lithification. Furthermore, lithoherms also grow in deep water, at depths that range between 600 and 800 m, well below the photic zone and storm wave base. Even though gas clathrate hydrates have not been identified with lithoherms, the water depth and temperature (5.5–10 °C) at the bottom of the Straits of Florida are conducive to their precipitation. It is tempting to suggest that the domal shape and relief of lithoherms above the surrounding bottom may, in part, be a result of heaving that would occur with subseafloor consolidation of gas clathrate hydrates.

Acknowledgements

Dr. A.J. Rowell gave me the chance to study the Meiklejohn Peak mud-mound; Dr. A. Limbird directed me to the literature on cryosoils; Mr. R.D. Malone provided a copy and photographs of his 1990 DOE report; Dr. M. Pope alerted me to recent geochemical work on the mud-mound; Drs. R. Bishnoi, R. Hyndman, H. Machiyama and K. Suyehiro pointed out the existence of carbon dioxide clathrate hydrates and Dr. H. Machiyama, in particular, referred me to the work of Sakai et al. (1990); Drs. G. Claypool, L. Hills, R. Koepnick, R. Meyer, K. Nuñez-Betelu, S. Sayegh and M. Tucker examined an earlier version of the manuscript; Dr. S. Sayegh for his friendship, support and discussions on gas clathrate hydrates; Drs. D. Haywick, D. Kopaska-Merkel and two anonymous referees reviewed the manuscript for Sedimentary Geology; Mr. J.C. Keeser (deceased) kindly drafted Figs. 1 and 2; Mr. J. Caswell assisted ably in the field and spent many hours experiencing the rigors of the Nevadan desert in July; Mr. S. Taylor and staff of the University of Calgary, Stable Isotope Laboratory; Ms. Regina Shedd of the Gallagher Library of Geology and Geophysics, University of Calgary, obtained references difficult to locate; the Beatty Public Library, Nevada, made their miniature Nevada oasis available; the American Association of Petroleum Geologists for a grant-in-aid of research; the Norcen Energy Resources for providing the Norcen Energy, Geology and Geophysics, Research Grant in Memory of Ms. Debbie Olsen; TotalFinaElf for providing access and support to the Centre Scientifique et Technique Jean Feger; and my family who have cheerfully and patiently supported my passion.

References

Aharon, P., Schwarcz, H.P., Roberts, H.H., 1997. Radiometric dating of submarine hydrocarbon seeps in the Gulf of Mexico. Geological Society of America Bulletin 109, 568–579.

Bathurst, R.G.C., 1959. The cavernous structure of some Mississippian Stromatactis reefs in Lancashire, England. Journal of Geology 67, 506–521.

Bathurst, R.G.C., 1971. Carbonate sediments and their diagenesis. Developments in Sedimentology, vol. 12. Elsevier, Amsterdam, 620 pp.

Bathurst, R.G.C., 1977. Ordovician Meiklejohn bioherm, Nevada. Geological Magazine 114, 308–311.

Bathurst, R.G.C., 1980. Stromatactis—origin related to submarine cemented crusts in Paleozoic mud-mounds. Geology 8, 131–134.

Bathurst, R.G.C., 1982. Genesis of stromatactis cavities between submarine crusts in Paleozoic carbonate mud buildups. Journal of the Geological Society of London 139, 165–181.

Beauchamp, B., Savard, M., 1992. Cretaceous chemosynthetic carbonate mounds in Arctic Canada. Palaios 7 (4), 434–450.

Bechstädt, T., 1974. Sind Stromatactis und radiaxialfibröser Calcit Faziesindikatorren. Neues Jahrbuch für Geologie und Paläontologie Monatshefte 11, 643–663.

Beskow, G., 1935. Soil-freezing and frost heaving with special applications to roads and railroads. In: Black, P.B., Hardenberg, M.J. (Eds.), Historical Perspectives in Frost Heave Research. The Early Works of S. Taber and G. Beskow United States Army Corps of Engineers, Cold Regions Research and Engineering Laboratory, Special Report 91–23, 169 pp.

Black, W.W., 1952. The origin of supposed tufa bands in Carboniferous knoll–reef limestones. Geological Magazine 89, 195–200.

Bohrmann, G.B., Greinert, J., Suess, E., Torres, M., 1998. Authigenic carbonates from the Cascadia subduction zone and their relation to gas hydrate stability. Geology 26, 647–650.

Booth, J.S., Winters, W.J., Dillon, W.P., Clennell, M.B., Rowe, M.M., 1998. Major occurrences and reservoir concepts in marine clathrate hydrates: implications of field evidence. In: Henriet, J.-P., Mienert, J. (Eds.), Gas Hydrates: Relevance to World Margin Stability and Climatic Change. Geological Society of London, Special Publication, vol. 137, pp. 113–127.

Bouriak, S.V., Akhmetjanov, A.H., 1998. Origin of gas hydrate accumulations on the continental slope of the Crimea from geophysical studies. In: Henriet, J.-P., Mienert, J. (Eds.), Gas Hydrates. Relevance to World Margin Stability and Climatic Change. Geological Society of London, Special Publication, vol. 137, pp. 215–233.

Bourque, P.-A., Boulvain, F., 1993. A model for the origin and petrogenesis of the Red Stromatactis Limestone of Paleozoic carbonate mounds. Journal of Sedimentary Petrology 63, 607–619.

Bourque, P.-A., Gignac, H., 1983. Sponge-constructed stromatactis mud mounds, Silurian of Gaspé, Québec. Journal of Sedimentary Petrology 53, 521–532.

Brock, R.D., Madigan, M.T., 1991. Biology of Microorganisms. Prentice-Hall, New Jersey, 874 pp.

Bunting, B.T., 1983. High Arctic soils through the microscope: prospect and retrospect. Annals of the Association of American Geographers 73, 609–616.

Bunting, B.T., Federoff, N., 1974. Micromorphological aspect of soil development in the Canadian High Arctic. In: Rutherford, G.K. (Ed.), Soil Microscopy. Proceedings of the 4th International Working Meeting on Soil Microscopy. Brown and Martin, Kingston, Ontario, Canada, pp. 350–364.

Carpenter, S.J., Lohmann, K.C., 1997. Carbon isotope ratios of Phanerozoic marine cements: re-evaluating the global carbon and sulfur systems. Geochimica et Cosmochimica Acta 61, 4831–4846.

Claypool, G.E., Kaplan, I.R., 1974. The origin and distribution of methane in marine sediments. In: Kaplan, I.R. (Ed.), Natural Gases in Marine Sediments. Marine Science, vol. 3. Plenum Press, New York, pp. 99–139.

Claypool, E., Kvenvolden, K.A., 1983. Methane and other hydrocarbon gases in marine sediment. Annual Review of Earth and Planetary Sciences 11, 299–327.

Cornwall, H.R., Kleinhampl, F.J., 1961. Geologic map of the Bare Mountain Quadrangle, Nevada. United States Geological Survey, Map GQ-157.

Dalziel, I.W., 1997. Neoproterozoic–Paleozoic geography and tectonics: review, hypothesis, environmental speculation. Geological Society of America Bulletin 109, 16–42.

Dupont, E., 1881. Sur l'origine des calcaires dévoniens de la Belgique. Bulletin de l'Academie Royal des Sciences Belgique 2, 264–280.

Finney, S.C., Ethington, R.L., 1995. Base of Whiterock Series correlates with base of Isograptus victoriae lunatus zone in Vinini Formation, Roberts Mountain, Nevada. In: Cooper, J.D., Drosser, M., Finney, S.C. (Eds.), Ordovician Odyssey: Short Papers for the 7th International Symposium on the Ordovician System. Pacific Section, Society for Sedimentary Geology (SEPM), Las Vegas, Nevada, pp. 153–156.

Friedman, I., O'Neil, J.R., 1977. Compilation of stable isotope fractionation factors of geochemical interest. United States Geological Survey, Professional Paper 440-KK, pp. 1–12.

Ginsburg, G.D., Soloviev, V.A., Cranston, R.E., Lorenson, T.D., Kvenvolden, K.A., 1993. Gas hydrates from the continental slope, offshore Sakhalin Island, Okhotsk Sea. Geo-Marine Letters 13, 41–48.

Harrison, W.E., Hesse, R., Gieskes, J.M., 1979. Relationship between sedimentary facies and interstitial water chemistry of slope, trench, and Cocos Plate sites from the Middle America Trench Transect, active margin off Guatemala, Deep Sea Drilling Project Leg 67. Initial Reports of the Deep Sea Drilling Project LXVII (67), 603–613.

Heckel, P.H., 1972. Possible inorganic origin for stromatactis in calcilutite mounds in the Tully Limestone, Devonian, of New York. Journal of Sedimentary Petrology 42, 7–18.

Hesse, R., 1990. Pore-water anomalies in gas hydrate-bearing sediments of the deeper continental margins: facts and problems. Journal of Inclusion Phenomena and Molecular Recognition in Chemistry 8, 117–138.

Hitchon, B., 1974. Occurrence of natural gas hydrates in sedimentary basins. In: Kaplan, I.R. (Ed.), Natural Gases in Marine Sediments. Marine Science, vol. 3. Plenum, New York, pp. 195–225.

Ivanov, M.K., Limonov, A.F., Woodside, J.M., 1998. Extensive deep fluid flux through the sea floor on the Crimean continental margin (Black Sea). In: Henriet, J.-P., Mienert, J. (Eds.), Gas Hydrates. Relevance to World Margin Stability and Climatic Change. Geological Society of London, Special Publication, vol. 137, pp. 195–213.

James, N.P., 1983. Reef environment. In: Scholle, P.A., Bebout, C.H., Moore, C.H. (Eds.), Carbonate Depositional Environments. American Association of Petroleum Geologists, Memoir, vol. 33, pp. 346–462.

Jenden, P.D., Gieskes, J.M., 1980. Chemical and isotopic composition of interstitial water from Deep Sea Drilling Project Sites 533 and 534. Initial Reports of the Deep Sea Drilling Project LXXVI (76), 453–461.

Johns, R.A., 1995. The good, the bad and the ugly: the paleoecology of Ordovician sponge/algal reef mounds. In: Cooper, J.D., Droser, M.L., Finney, S.C. (Eds.), Ordovician Odyssey: Short Papers for the 7th International Symposium on the Ordovician System. Pacific Section, Society for Sedimentary Geology (SEPM), Fullerton, pp. 429–433.

Katz, D.L., Cornell, D., Kobayashi, R., Poettman, F.H., Vary, J.A., Elenbaas, J.R., Weinaug, C.F., 1959. Chapter 5: Water–Hydrocarbon systems. Handbook of Natural Gas Engineering. McGraw-Hill, New York, p. 802.

Kaufmann, B., 1998. Middle Devonian reef and mud mounds on a carbonate ramp: Mader Basin (eastern Anti-Atlas, Morocco). In: Wright, V.P., Burchette, T.P. (Eds.), Carbonate Ramps. Geological Society of London, Special Publication, vol. 149, pp. 417–435.

Krause, F.F., 1974. Systematics and distributional patterns of inarticulate brachiopods on the Ordovician carbonate mud-mound at Meiklejohn Peak, Southwestern Nevada. MSc Thesis, University of Kansas, Lawrence, 283 pp.

Krause, F.F., 1999. Genesis of a mud-mound, Meiklejohn Peak, Nevada, USA. 11th Bathurst Meeting, Journal of Conference Abstracts, Cambridge, UK, vol. 4 (2), 941.

Krause, F.F., 2000. Clathrate hydrate frost heave structures in a carbonate mud-mound: Meiklejohn Peak, Nevada, USA. American Association of Petroleum Geologists, Annual Convention, Official Program, vol. 9, A81.

Krause, F.F., Rowell, A.J., 1975. Distribution and systematics of the inarticulate brachiopods of the Ordovician carbonate mud-mound of Meiklejohn Peak, Nevada. Paleontological Contributions. The University of Kansas, Lawrence, KS, USA, Article 61, p. 74.

Krause, F.F., Sayegh, S.G., 2000. Cool/cold water carbonates, mud-mounds and methane clathrate hydrates: fuelling the

new millennium. Canadian Society of Petroleum Geologists, Reservoir 27 (6), 10.

Kvenvolden, K.A., 1998. A primer on the geological occurrence of gas hydrate. In: Henriet, J.-P., Mienert, J. (Eds.), Gas Hydrates. Relevance to World Margin Stability and Climatic Change. Geological Society of London, Special Publication, vol. 137, pp. 9–30.

Lees, A., 1964. The structure and origin of the Waulsortian (Lower Carboniferous) "reefs" of west-central Eire. Philosophical Transactions of the Royal Society of London, Series B 247, 483–531.

Lees, A., Miller, J., 1995. Waulsortian banks. In: Monty, C.V.L., Bosence, D.W.J., Bridges, P.H., Pratt, B.R. (Eds.), Carbonate Mud-Mounds. Their Origin and Evolution. International Association of Sedimentologists, Special Publication, vol. 23, pp. 191–271.

Logan, B.W., Semeniuk, V., 1976. Dynamic metamorphism: processes and products in Devonian carbonate rocks, Canning Basin, Western Australia. Geological Society of Australia, Special Publication, vol. 6, pp. 1–138.

MacDonald, I.R., Guinasso Jr., N.L., Sassen, R., Brooks, J.M., Lee, L., Scott, K.T., 1994. Gas hydrate that breaches the sea floor on the continental slope of the Gulf of Mexico. Geology 22, 699–702.

Malone, R.D., 1990. Gas hydrates. DOE/METC-90/0270(DE 90015321), United States Department of Energy, Morgantown Energy Technology Center, Morgantown, WV, 52 pp.

Miller, S.L., 1974. The nature and occurrence of clathrate hydrates. In: Kaplan, I.R. (Ed.), Natural Gases in Marine Sediments, vol. 3. Plenum, New York, pp. 151–177.

Monty, C.L.V., 1995. The rise and nature of carbonate mud-mounds: an introductory actualistic approach. In: Monty, C.L.V., Bosence, D.W.J., Bridges, P.H., Pratt, B.R. (Eds.), Carbonate Mud-Mounds. Their Origin and Evolution. International Association of Sedimentologists, Special Publication, vol. 23, pp. 11–48.

Mounji, D., Bourque, P.-A., Savard, M.M., 1998. Hydrothermal origin of Devonian conical mounds (Kess–Kess) of Hamar Lakhdad Ridge, Anti-Atlas, Morocco. Geology 26, 1123–1126.

Mullins, H.T., Neumann, A.C., Wilber, R.J., Hine, A.C., Chinburg, S.J., 1980. Carbonate sediment drifts in Northern Straits of Florida. American Association of Petroleum Geologists Bulletin 64, 1701–1717.

Neumann, A.C., Kofoed, J.W., Keller, G.H., 1977. Lithoherms in the Straits of Florida. Geology 5, 4–10.

Orange, D.L., Green, H.G., Reed, D., Martin, J.B., McHugh, C.M., Ryan, W.B.F., Maher, N., Stakes, D., Barry, J., 1999. Widespread fluid expulsion on a translational continental margin: Mud volcanoes, fault zones, headless canyons and organic-rich substrate in Monterey Bay, California. Geological Society of America Bulletin 111, 992–1009.

Orme, G.R., Brown, W.W.M., 1963. Diagenetic fabrics in the Avonian limestones of Derbyshire and North Wales. Proceedings of the Yorkshire Geological Society 34, 51–66.

Philcox, M.E., 1963. Banded calcite mudstone in the Lower Carboniferous "reef" knolls of the Dublin basin, Ireland. Journal of Sedimentary Petrology 33, 904–913.

Pratt, B.R., 1982. Stromatolitic framework of carbonate mudmounds. Journal of Sedimentary Petrology 52, 1203–1227.

Pratt, B.R., 1995. The origin, biota and evolution of deep-water mud-mounds. In: Monty, C.L.V., Bosence, D.W.J., Bridges, P.H., Pratt, B.R. (Eds.), Carbonate Mud-Mounds. Their Origin and Evolution. International Association of Sedimentologists, Special Publication, vol. 23, 49–123.

Presley, B.J., Kaplan, I.R., 1968. Changes in dissolved sulfate, calcium and carbonate from interstitial water of near-shore sediments. Geochimica et Cosmochimica Acta 32, 1037–1048.

Reitner, J., Neuweiler, F., Flajs, G., Vigener, M., Keupp, H., Meischner, D., Neuweiler, F., Paul, J., Reitner, J., Warnke, K., Weller, H., Dingle, P., Hensen, C., Schäfer, P., Gautret, P., Leinfelder, R.R., Hüssner, H., Kaufmann, B., 1995. Mud-mounds: a polygenetic spectrum of fine-grained carbonate buildups. Facies 32, 1–70.

Roberts, H.H., Carney, R.S., 1997. Evidence of episodic fluid, gas, and sediment venting on the Northern Gulf of Mexico continental slope. Economic Geology 92, 863–879.

Roberts, H.H., Aharon, P., Walsh, M.M., 1992. Cold-seep carbonates of the Louisiana Continental Slope-to-Basin Floor. In: Rezak, R., Lavoie, D. (Eds.), Carbonate Microfabrics. Springer-Verlag, Berlin, pp. 95–104.

Romans, J.C.C., Robertson, L., 1974. Some aspects of the genesis of alpine and upland soils in the British Isles. In: Rutherford, G.K. (Ed.), Soil Microscopy. Proceedings of the 4th International Working Meeting on Soil Microscopy. Brown and Martin, Kingston, Ontario, Canada, pp. 498–510.

Romans, J.C.C., Robertson, L., Dent, D.L., 1980. The micromorphology of young soils from South-East Iceland. Geographical Annals 62, 93–103.

Ross Jr., R.J., 1964. Middle and Lower Ordovician formations in southernmost Nevada and California. United States Geological Survey, Bulletin 1180C, C1–C101.

Ross Jr., R.J., 1972. Fossils from the Ordovician bioherm at Meiklejohn Peak, Nevada. United States Geological Survey, Professional Paper 685, 47 pp.

Ross Jr., R.J., Cornwall, H.R. 1961. Bioherms in the upper part of the Pogonip in southwestern Nevada. United States Geological Survey, Paper 424-B, B231–B233.

Ross Jr., R.J., Ethington, R.L. 1991. Stratotype of the Ordovician Whiterock Series. Palaios 6 (2), 156–173.

Ross Jr., R.J., Jaanusson, V., Friedman, I. 1975. Lithology and origin of Middle Ordovician calcareous mud-mound at Meiklejohn Peak, Southern Nevada. United States Geological Survey, Professional Paper 871, 48 pp.

Ross Jr., R.J., James, N., Hintze, L.F., Poole, F.G. 1989. Architecture and evolution of a Whiterockian (Early Middle Ordovician) carbonate platform, Basin Ranges of western USA. In: Crevello, P.D., Wilson, J.L., Sarg, J.F., Read, J.F. (Eds.), Controls on Carbonate Platform and Basin Development. Society for Sedimentary Geology (SEPM), Special Publication, vol. 44, pp. 167–185.

Sakai, H., Gamo, T., Kim, E.-S., Tsutsumi, M., Tanaka, T., Ishibashi, J., Wakita, H., Yamano, M., Oomori, T., 1990. Venting of carbon dioxide-rich fluid and hydrate formation in Mid-Okinawa Trough Backarc Basin. Science 248, 1093–1096.

Sassen, R., MacDonald, I.R., Guinaso Jr., N.L., Joye, S., Requejo, A.G., Sweet, S.T., Alcalá-Herrera, J., DeFreitas, D.A., Schink, D.R., 1998. Bacterial methane oxidation in sea-floor gas hydrate: significance to life in extreme environments. Geology 26, 851–854.

Schwarzacher, W., 1961. Petrology and structure of some Lower Carboniferous reefs in northwestern Ireland. American Association of Petroleum Geologists Bulletin 45, 1481–1503.

Shinn, E.A., 1968. Burrowing in Recent lime sediments of Florida and the Bahamas. Journal of Paleontology 40, 879–894.

Sloan, E.D.J., 1998a. Clathrate Hydrates of Natural Gases. Marcel Dekker, New York, 705 pp.

Sloan, E.D.J., 1998b. Physical/chemical properties of gas hydrates and applications to world margin stability and climatic change. In: Henriet, J.-P., Mienert, J. (Eds.), Gas Hydrates. Relevance to World Margin Stability and Climatic Change. Geological Society London, Special Publication, vol. 137, pp. 31–50.

Sprinkle, J., Guensberg, T.E., 1995. Origin of echinoderms in Paleozoic evolutionary fauna: the role of substrates. Palaios 10 (5), 437–453.

Suess, E., Bohrmann, G., Greinert, J., Lausch, E., 1999. Flammable ice. Scientific American 281 (5), 76–83.

Taber, S., 1929. Frost heaving. Journal of Geology 37, 429–461.

Taber, S., 1930. The mechanics of frost heaving. Journal of Geology 38, 303–317.

Thurman, H.V., 1988. Introductory Oceanography. Merrill, Columbus, OH, 515 pp.

Tobin, K.J., Walker, K.R., 1995. Meiklejohn Peak's fibrous calcite: implications for the Ordovician $\delta^{18}O$ marine record. In: Cooper, J.D., Drosser, M., Finney, S.C. (Eds.), Ordovician Odyssey: Short Papers for the 7th International Symposium on the Ordovician System. Pacific Section, Society for Sedimentary Geology (SEPM), Las Vegas, Nevada, pp. 385–388.

Tucker, M.E., 1983. Diagenesis, geochemistry, and origin of a Precambrian dolomite: the Beck Spring Dolomite of Eastern California. Journal of Sedimentary Petrology 53, 1097–1119.

Veizer, J., Bruckschen, P., Pawellek, F., Diener, A., Podhala, O.G., Carden, G.A.F., Jasper, T., Korte, C., Strauss, H., Azmy, K., Ala, D., 1997. Oxygen isotope evolution of Phanerozoic seawater. Palaeogeography, Palaeoclimatology, Palaecology 132, 159–172.

Wendt, J., Kaufmann, B., 1998. Mud buildups on a Middle Devonian carbonate ramp (Algerian Sahara). In: Wright, V.P., Burchette, T.P. (Eds.), Carbonate Ramps. Geological Society of London, Special Publication, vol. 149, pp. 397–415.

Wendt, J., Zdzislaw, B., Kaufman, B., Kostrewa, R., Hayer, J., 1997. The world's most spectacular carbonate mud mounds (Middle Devonian, Algerian Sahara). Journal of Sedimentary Research 67, 424–436.

Wolf, K.H., 1965. Littoral environment indicated by open-space structures in algal limestones. Palaeogeography, Palaeoclimatology, Palaeoecology 1, 183–223.